DIELECTRIC RESPONSE ANALYSIS FOR CONDITION ASSESSMENT OF XLPE POWER CABLE

A Thesis Submitted in Partial Fulfilment for the Degree of Master of Electrical Engineering

By

ARUP KUMAR DAS

Examination Roll No.: **M4ELE19014**

Registration No. : **140658 of 2017-18**

Under the guidance of

Dr. Abhijit Mukherjee

Professor

&

Dr. Sovan Dalai

Associate Professor

Department of Electrical Engineering

Faculty of Engineering and Technology

Jadavpur University

Kolkata, India

JADAVPUR UNIVERSITY

KOLKATA- 700032, INDIA

FACULTY OF ENGINEERING AND TECHNOLOGY

CERTIFICATE OF RECOMMENDATION

This is to certify that the thesis entitled "**Dielectric Response Analysis for Condition Assessment of XLPE Power Cable**" is being submitted by Arup Kumar Das (Registration No. 140658 of 2017-18), in partial fulfilment of the requirement for the degree of "Master of Electrical Engineering" from Jadavpur University has been carried out by him under our guidance and supervision. The project, in our opinion, is worthy of its acceptance.

Dr. Abhijit Mukherjee

Professor,

Dept. of Electrical Engineering,

Faculty of Engineering and Technology,

Jadavpur University

Dr. Sovan Dalai

Associate Professor,

Dept. of Electrical Engineering,

Faculty of Engineering and Technology,

Jadavpur University

Prof. Kesab Bhattacharyya

Head, Dept. of Electrical Engineering,

Faculty of Engineering and Technology,

Jadavpur University

Prof. Chiranjib Bhattacharjee

Dean,

Faculty of Engineering and Technology,

Jadavpur University

JADAVPUR UNIVERSITY

KOLKATA- 700032, INDIA

FACULTY OF ENGINEERING AND TECHNOLOGY

CERTIFICATE OF APPROVAL

The foregoing thesis is hereby approved as a credible study of Master of Electrical Engineering and presented in a manner satisfactory to warrant its acceptance as a prerequisite to the degree for which it has been submitted. It is understood that by this approval the undersigned do not necessarily endorse or approve any statement made, opinion expressed or conclusion therein but approve this thesis only for the purpose for which it is submitted.

1. _____

_____ 2. _____

Signature of the Examiner(s) Signature of the Supervisors

*Only in case the recommendation is concurred in

DECLARATION OF ORIGINALITY AND COMPLIANCE OF ACADEMIC ETHICS

I hereby declare that the thesis entitled "**Dielectric Response Analysis for Condition Assessment of XLPE Power Cable**" contains literature survey and original research work as part of the course of Master of Engineering studies. All the information in this document has been obtained and presented in accordance with academic rules and ethical conduct.

I also declare that, as required by these rules and conduct, I have fully cited and referenced all material and results that are not original to this work.

Name (Block Letters)	:	ARUP KUMAR DAS
Exam Roll no.	:	M4ELE19014
Registration no.	:	140658 of 2017-18
Thesis Name	:	DIELECTRIC RESPONSE ANALYSIS FOR CONDITION ASSESSMENT OF XLPE POWER CABLE
Signature with date	:	

ACKNOWLEDGEMENT

I express my deep sense of gratitude to my supervisors, **Dr. Abhijit Mukherjee**, Professor, Department of Electrical Engineering, Jadavpur University and **Dr. Sovan Dalai,** Associate Professor, Department of Electrical Engineering, Jadavpur University for their keen interest, cherished guidance and constant inspiration during the course of the research work. I am obliged and grateful to them for their guidance and giving the opportunity to work in the High Tension Laboratory. Above all, without their moral support and constant guidance, I would not have completed the work.

I express my sincere gratitude to **Prof. Kesab Bhattacharyya** and **Dr. Biswendu Chatterjee,** Department of Electrical Engineering, Jadavpur University, for their encouragement, advice and active support in this work. I owe a debt of gratitude to **Dr. Arpan Kumar Pradhan**, Department of Electrical Engineering, Jadavpur University, for his continuous guidance, maverick ideas and. He also worked equally hard to make this work reach its conclusion and beyond. I also convey special thanks to the **High Tension Laboratory** of Jadavpur University, Kolkata, for providing facility and support during this research work.

I am also thankful to **Prof. Kesab Bhattacharyya**, Head, Department of Electrical Engineering, Jadavpur University, for providing the necessary facilities for carrying out this research work.

I am taking the opportunity to express my humble indebtedness to **Mr. Nasirul Haque** and **Mr. Biswajit Chakraborty**, research scholar, High Tension Laboratory, for their invaluable inputs during this work. I am also thankful to rest of the research scholars of High Tension laboratory for their support throughout the tenure of the research work.

I would like to thank my dear friend **Miss. Payel Banerjee**, PG scholar, E.E. Department, from whom I received immense support, inexplicable encouragements and assistance. I would like to convey my soulful thankfulness to the rest of the PG scholars of E.E. Department for their moral support during this course work. I am extremely grateful to my parents and my sister for their constant support and motivation, without that I would not have come to this stage. This thesis, a fruit of the combined efforts of my family members, is dedicated to them as a token of love and gratitude.

Above all, it is the wish of the almighty that I have been able to complete this work.

Date: Arup Kumar Das

DEDICATED TO MY PARENTS

CONTENTS

ABSTRACT	I
NOMENCLATURE	II-IV
CHAPTER-1: **INTRODUCTION**	1-5
1.1. INTRODUCTION	2
1.2. AIM OF THE THESIS	3
1.3. CONTENT OF THE THESIS	3
1.4. ORGANIZATION OF THE THESIS	4
CHAPTER-2: **INSULATION AND DIAGNOSTICS METHOD**	6-12
2.1.INTRODUCTION	7
2.2.ADVANTAGES OF XLPE INSULATION IN UNDERGROUND CABLE SYSTEM	8
2.3. DEGRADATION PROCESS OF XLPE INSULATION	8
2.3.1.THERMAL DEGRADATION	9
2.3.2.CHEMICAL DEGRADATION	9
2.3.3.ELECTRICAL DEGRADATION	10
2.3.4.WATER TREEING	10
2.3.5.ELECTRICAL TREEING AND PARTIAL DISCHARGE	11
2.4.DIAGNOSTICS METHOD	11
CHAPTER-3: **THEORY OF DIELECTRIC RESPONSE**	13-22

ANALYSIS

3.1. INTRODUCTION 14

3.2. DIELECTRIC RESPONSE MEASUREMENT METHOD 14

3.3. TIME DOMAIN SPECTROSCOPY 15

3.3.1.POLARIZATION AND DEPOLARIZATION CURRENT MEASUREMENT 17

3.3.2.PDC MEASUREMENT FLOWCHART 19

3.3.3.ADVANTAGES OF PDC MEASUREMENT 20

3.3.4.LIMITATIONS OF PDC MEASUREMENT 20

3.4. FREQUENCY DOMAIN SPECTROCOPY 20

3.4.1.ADVANTAGES OF FDS MEASUREMENT 22

CHAPTER-4: **EXPERIMENTAL STUDY** 23-31

4.1.INTRODUCTION 24

4.2.SPECIFICATIONS OF CABLE 24

4.3.SAMPLE PREPARATION USING XLPE CABLE 25

4.4.EQUIPMENTS EMPLOYED 25

4.4.1.THERMAL OVEN 25

4.4.2.THE DIRANA 26

4.4.3.THE IDAX 27

4.4.4.LCR METER 27

4.5.EXPERIMENTAL PROCEDURE 28

CHAPTER-5: **RESULT AND DISCUSSION** 32-40

5.1. INTRODUCTION 33

5.2. VALUE OF GEOMETRIC CAPACITANCE 33

5.3. COMPARATIVE STUDY OF PDC MEASUREMENT 33

5.4. COMPARATIVE STUDY OF FDS MEASUREMENT 36

CHAPTER-6: **MODELING OF XLPE CABLE INSULATION** 41-50

6.1. INTRODUCTION 42

6.2. CALCULATION OF MODEL PARAMETERS 43

6.3. PROCEDURE AND FLOWCHART OF PDC MEASUREMENT MODELLING 43

6.4. ESTIMATED RESULT OF DEBYE MODEL BRANCH PARAMETERS 46

6.5. DISCUSSION 49

6.6. ADVANTAGES AND DRAWBACKS 50

CHAPTER-7**: DIELECTRIC RELAXATION CHARACTERISTICS OF XLPE CABLE INSULATION** 51-67

7.1. INTRODUCTION 52

7.2. DIELECTRIC RELAXATION MODELS 52

7.2.1.DEBYE-MODEL OF DIELECTRIC RELAXATION 52

7.2.2.COLE – COLE MODEL & COLE-DAVIDSION MODEL 53

7.2.3.HAVRILIAK-NEGAMI (H-N) RELAXATION MODEL 54

7.3. GRAPHICAL METHOD OF HAVRILIAK–NEGAMI PARAMETER CALCULATION 55

7.4. FITTING OF MODEL PARAMETERS AND RESULT 57

7.4.1.OPERATING TEMPERATURE VARIATION 57

7.4.2.WATER CONTENT VARIATION 62

7.5. CONCLUSION 67

CHAPTER-8: **ESTIMATION OF WATER CONTENT IN XLPE CABLE** 68-71

8.1. INTRODUCTION 69

8.2. ESTIMATED RESULT OF WATER CONTENT 69

8.3. CONCLUSION 71

CHAPTER-9: **CONCLUSION AND FUTURE SCOPE** 72-74

9.1. CONCLUSION 73

9.2. FUTURE SCOPE 74

REFERENCES 75-78

ABSTRACT

In recent times, there has been a growing thrust on bulk power transmission through long distances. This has led to higher operating voltage levels for power transmission. As a result, transformers, cables and other power equipments have to go through higher operating stresses. The lifetime of power equipment directly depends on the condition of insulation. Most of the high voltage (HV) power equipment use solid insulation like paper insulation, glass insulation, epoxy insulation etc. Among all the insulation materials, paper insulation has long been used in cable and nowadays the commonly used insulating material is Cross linked Polyethylene (XLPE). Power cables operate underground for several years and many factors like moisture, temperature can affect cable insulation over the years. The presence of impurities in the insulation system is one of the root causes of insulation failure, as they form a weak zone inside the healthy insulation system. Therefore, early identification of the degradation processes like formation of water tree structures inside such solid insulation due to high voltage stress during its operating life, is of utmost importance to prevent the power equipment from a sudden and complete insulation failure, as any kind of failure leads to economic losses and other problems. Dielectric response analysis is one of the advanced tools for the condition monitoring of cable insulation. Since, only breakdown strength does not reflect performance and suitability of a insulation for practical application, a thorough investigation of dielectric properties of insulation is necessary to comment on its suitability in practical applications. To study the dielectric properties of XLPE cable insulation, time domain spectroscopy and frequency domain spectroscopy methods are applied in this work. This work is aimed to study the effect of operating temperature and water content inside the insulation due to water tree aging on XLPE cable. To study the effect of operating temperature and water content on XLPE cable, an equivalent circuit model has been proposed through PDC measurement. This work describes effect of temperature and water content on dielectric relaxation characteristics of XLPE cable, through Havriliak – Negami relaxation model employing frequency domain spectroscopy data. This thesis also proposes a methodology to estimate water content inside the insulation through dielectric spectroscopy data.

NOMENCLATURE

D	Electric flux density
E	Electric field
ε_0	Permittivity of vacuum
ε_r	Relative permittivity of an insulating material
P	Polarization vector
χ	Electrical susceptibility of a dielectric material
U_0	Step voltage source
$\delta(t)$	Dirac function/delta function
ε_s	Static relative permittivity
ε_∞	High frequency relative permittivity
χ_s	Static electrical susceptibility
χ_∞	High frequency susceptibility
J	Displacement current density
σ_0	DC conductivity
C_0	Geometric capacitance
$f(t)$	Polarization function
i_{pol}	Polarization current
i_{depol}	Depolarization current
ω	Frequency of applied voltage

$\hat{\chi}(\omega)$	Complex susceptibility of the sample
$\chi'(\omega)$	Real part of complex susceptibility
$\chi''(\omega)$	Imaginary part of complex susceptibility
$C'(\omega)$	Real part of complex capacitance
$C''(\omega)$	Imaginary part of the complex capacitance
ε'_r	Real part of relative permittivity
ε''_r	Imaginary part of relative permittivity
$\tan\delta$	Dielectric dissipation factor
A_i	Branch current
τ_i	Time constant of R-C branches
R_0	Insulation resistance
R_i	Branch resistance of Debye model
C_i	Branch capacitance of Debye model
τ_d	Debye relaxation time constant
τ_{cc}	Cole-Cole relaxation time constant
τ_{cd}	Cole-Davidson relaxation time constant
α	Distribution parameter in Haviriliak-negami model
β	Symmetry parameter in Haviriliak-negami model
φ_l	Angle made by the slope of straight line in Havriliak –negami plot
τ_{hn}	Haviriliak-negami relaxation time constant

a_i, b_i	Coefficients of fitting parameters
t	Operating temperature in °C
$\tan\delta_{pwr}$	Dissipation factor at power frequency region
$\tan\delta_{min}$	Minimum dissipation factor in FDS curve
k_1, k_2	Coefficients for estimating water content inside cable insulation
θ_w	Volumetric Water content inside the insulation in ppm
V_w	Volume of injected water
V_i	Volume of XLPE insulation

Numbering of Figures, Tables and Equations

Figures, tables and equations have been numbered in accordance with the chapters in which they appear in the thesis. Each figure, table and equation has two distinct numbers. The first one specifies the number of the chapter and the second number denotes to the actual number of the figure, table and equation in that chapter.

Representation of References

The list of references has been furnished at the end of the thesis. These references has been represented by the respective name of the author(s) along the year of publication.

CHAPTER-1

INTRODUCTION

CHAPTER-1

1.1.INTRODUCTION:

Electrical power transmission and distribution systems include a large number of important and expensive underground power cable systems of different age manufactured and installed over many decades. These power cables are the assembly of some conductors bundled together covered with insulating material and protective jackets. The insulation is either made up of thermoplastic compound, thermosetting compound or oil-paper. The oldest oil-paper insulated power cables still in use, were installed in the 1940s. Installation of XLPE-cables had been started in the middle of the 1970s.

For reliability purposes, quantitive measurement on certain components in the HV power equipment should be taken. Repair and replacement of faulty part in underground cable systems are expensive and correct timing in these activities can leads to large savings in costs. Condition based monitoring of underground cable system is thus becoming more common for economic reasons. The insulation systems of underground power cables are subject to different kinds of stresses (electrical, mechanical, thermal) during their service life and thus suffer deterioration and degradation. These can lead to breakdown or failure of system, which in turn reduces the reliability of electrical transmission and distribution systems. Therefore, a lot of research activities are directed towards a better understanding of degradation process, development of tools for insulation diagnosis and the establishment of remaining lifetime estimation techniques. In order to check the quality and reliability of a cable system, it is important to perform diagnostic tests before putting the cable system into service and after a certain period of operation. On-site insulation diagnosis to detect the aging and degradation status of power equipment is of great interest within the power and grid companies and utilities [1-3].

It is impossible to carry out diagnostics tests on all cable systems in service. It is even harder to carry out full laboratory-scale testing of each cable system in service. Therefore, there is a point in collecting samples of cable insulation for experimental analysis. Analyzed results can provide useful information about the actual condition of the cable insulation.

Several diagnostics tools are used for condition assessment of power cables. Among them, Dielectric response analysis is one of the popular and non-destructive tool for condition monitoring of power cable insulation. Based on the theory of dielectric

polarization there are 3 methods for dielectric response analysis given as follows, 1) PDC (Polarization Depolarization Current measurement) 2) FDS (Frequency Domain Spectroscopy) 3) RVM (Recovery Voltage Measurement).

In this thesis, PDC & FDS tools are applied for condition monitoring of XLPE cable. Time domain spectroscopy or PDC observes polarization characteristics of the insulation whereas Frequency domain spectroscopy observes dielectric dissipation factor which reflects the losses of the dielectric medium.

1.2.AIM OF THE THESIS

Two fully automatic instruments DIRANA and IDAX have been used for quantitative measurement of dielectric response of XLPE cable insulation. DIRANA has been used to measure and investigate polarization and depolarization current whereas IDAX is employed to measure real and imaginary capacitance and dissipation factor of the insulation at wide range of frequency.

The aim of the thesis is to monitor the effect of operating temperature and migrated water variation inside polymeric insulation by analysing active polarization process in polymeric dielectric. Based on Polarization Depolarization current (PDC) data an equivalent electrical circuit model (Debye Model) of the insulation system has been simulated to access the active polarization process of the dipoles present in polymeric dielectric. Debye model has certain limitations as it is applicable to linear dielectrics. As polymeric insulations are amorphous solid, they don't obey Debye relaxation, so a new model (Harviliak-Negami relaxation model) has been proposed based on FDS data to investigate the effect of temperature and water content on relaxation characteristics of the dipoles present inside XLPE cable insulation. This thesis is also aimed at predicting the amount of accumulated water inside XLPE cable insulation employing dielectric spectroscopy data.

1.3.CONTENT OF THE THESIS:

The whole project is divided into 2 parts, the 1st part is related to operating temperature variation and the 2nd part to variation of accumulated water content inside cable insulation. The main objectives of this work are:

- To conduct a comparative study on the polarization & depolarization curves of XLPE cable at different operating temperature and accumulated water content inside the insulation.
- To conduct comparative studies on the parameters like complex permittivity and the dielectric dissipation factor of XLPE cable at different operating temperature and accumulated water content.
- To simulate an equivalent electrical circuit model of XLPE cable insulation based on measured PDC curve and study the variation of time constants and estimate the R-C branch parameters with operating temperature and water content.
- To investigate dielectric relaxation characteristics of XLPE cable insulation through Havriliak–Negami model employing frequency domain spectroscopy (FDS) data.
- To study the variation of Havriliak–Negami relaxation parameters like distribution parameter (α), symmetry parameter (β) and relaxation time constant (τ_{hn}) with operating temperature and water content.
- To estimate accumulated water content inside the insulation of XLPE cable employing Frequency domain spectroscopy (FDS) data.

1.4.ORGANIZATION OF THE THESIS:

The entire thesis work is documented in nine separate chapters as follows:

Chapter 1 explains background, aim of the thesis and contents of the thesis work.

Chapter 2 elucidates the degradation process of XLPE cable, it also describes diagnostics methods for condition monitoring of XLPE cable.

Chapter 3 explains the brief theory of dielectric spectroscopy in both time and frequency domain.

Chapter 4 provides the experimental details involved in the present work which includes sample preparation and experimental procedure.

Chapter 5 presents the results of the experiment and the comparative analysis that were done on the basis of those results.

Chapter 6 describes the equivalent circuit modeling of XLPE cable insulation based on PDC measurement. It also shows this variation of model parameters with operating temperature and water content.

Chapter 7 provides basic idea about different dielectric relaxation models. This chapter also describes dielectric relaxation characteristics of XLPE cable insulation for different operating temperature and water content, based on Havriliak-Negami relaxation model.

Chapter 8 proposes a technique to predict accumulated water content inside XLPE cable, employing dielectric spectroscopy data.

Chapter 9 provides the conclusions and also briefly discusses the scope for future work.

CHAPTER-2

INSULATION AND DIAGNOSTIC METHOD

CHAPTER-2

2.1.INTRODUCTION:

Cross Linked Polyethylene or XLPE insulated power cables are used increasingly since the end of 1960s. All the new installation and repairing of existing underground cable system are performed using XLPE cable. A schematic diagram of 1-core 11KV XLPE cable has been shown in Fig. 2.1.

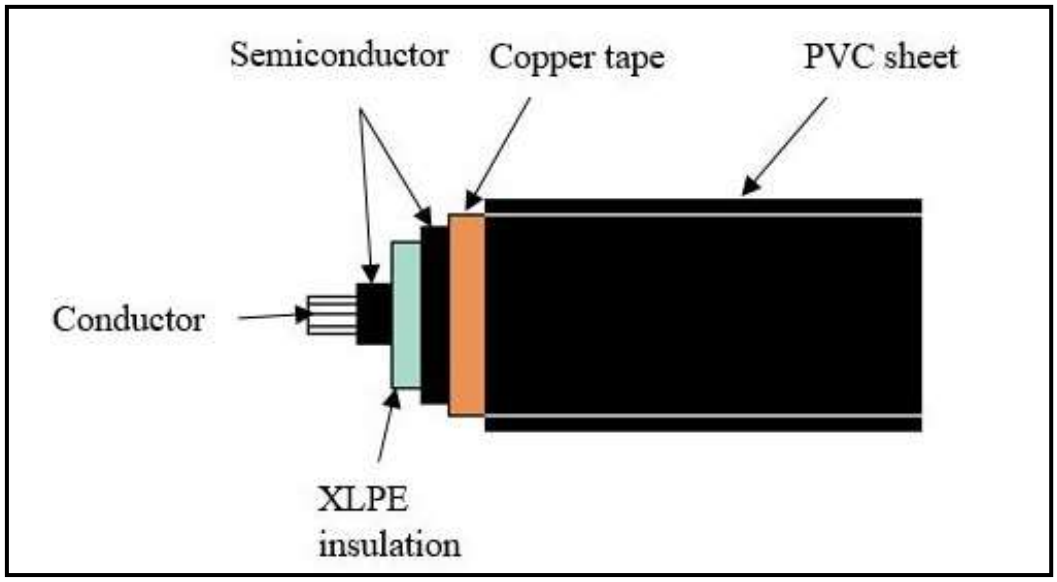

Fig. 2.1. Schematic diagram of 1-core XLPE cable

The basic material of XLPE is LDPE (Low-Density Polyethylene). It is a semi-crystalline polymer and produced by the polymerization process of ethylene (C_2H_4). Cross-linking agents like dicumyl peroxide (DCP), trimethylolpropane (TMPTA) give rise to Cross-linked polyethylene (XLPE). An insulating material is shaped over conductor by triple extrusion. During this process, polyethylene is mixed with a crosslinking agent. Temperature kept during this process is around 130ºC. After the extrusion process, the insulated core is going through a tube filled with heated and pressurised N_2 gas for vulcanisation Cross-linking process leads polyethylene from thermoplastic to thermosetting material with improved mechanical and electrical properties. During vulcanisation, crosslinking agents are decomposed into reactive primary radicals due to heat and pressure, which affect the cross-linking [4].

The cable is cooled down afterwards. This period can cause residual mechanical stresses inside the insulation, which may not be uniformly distributed inside the insulation.

Residual mechanical stresses during the manufacturing process have an impact on the breakdown strength of cable insulation [5].

During the manufacturing process cross-linking by-products are formed. Water is formed during crosslinking of polyethylene. At the meantime acetophenone and cumyl alcohol are also formed in the quantity of 1% weight of the fresh vulcanised insulation. Up to 99.5 % of the cross-linking by-products will be consumed during the curing process. After degassing the insulation, the residual cross-linking by-products will be less than 4000 ppm and the water by-product should be less than 150 ppm [6]. The longevity and quality of XLPE cable can be improved by using additives during manufacturing process. Additives can enhance water tree retardant capabilities. Antioxidants are blended into the insulation to capture highly reactive and harmful free-radicals [5].

2.2.ADVANTAGES OF XLPE INSULATION IN UNDERGROUND CABLE SYSTEM:

- **Excellent mechanical and electrical properties:** XLPE has great electrical and mechanical properties. So, it is considered as the most preferable insulating material for medium voltage and high voltage power cable.
- **High temperature withstand capability:** XLPE can withstand high temperature compared to LDPE & HDPE. The maximum operating temperature of XLPE cable is 90ºC while conventional PE cable to be used that of 75ºC. During short circuit, XLPE cable can be operated temperature up to 120ºC for a very short time period [7].
- **No Metallic Sheath Required:** XLPE does not soak water, hence no metallic casing required. So, it is free from metallic sheath failures such as corrosion or wear and tear of the casing.
- **Ease of Installation:** XLPE is light in weight and the process of installation is simple, the termination process is also simpler compared to other cables.

2.3.DEGRADATION PROCESS OF XLPE INSULATION:

The degradation process of XLPE cable can be divided into 2 parts i.e. extrinsic degradation process and intrinsic degradation process. Extrinsic degradation process is mainly due to voids or micro-pores and contaminated particle present inside the cable insulation. Whereas, intrinsic degradation is due to any change in the chemical or physical property of the insulation or due to the trapped charges [8]. Intrinsic degradation is not restricted to a local area but it affects the large volume of the insulation, like chemical or

thermal degradation affects a large portion of the cable. Polymers cannot achieve final crystal structure right after manufacturing, as curing is a slow process. Therefore, micro-cavities and locally denser areas can be created inside the insulation [9].

Polyethylene (PE) consists of spherulites, which is formed during crystallisation. Diameters of spherulites are normally more than 10 micrometres. For XLPE, structure of spherulite is usually weaker and replaced by lamellar stacks. XLPE consists of two main parts, spherulites and the amorphous region. In XLPE there exist many micro-interfaces between spherulites and the amorphous region due to contaminated particles or water-filled micro-pores. Contaminated particles are generally residual cross-linking by-products or antioxidant. Water filled micro-pores formed due to water by-product usually in XLPE [5].

2.3.1. THERMAL DEGRADATION:

Under normal condition, the operating temperature of XLPE cable should be within 90ºC, though cables can be operated at temperature up to 120 ºC during faulty condition. At a temperature ranging 150ºC -225ºC, free radicals can attach to the other polymer chains may result in the decrement of mechanical strength, density and crystallinity. If the temperature is increased beyond 225ºC, trans-vinyl groups are formed which indicates radical rearrangements. At a very high temperature beyond 350ºC polyethylene degrades through depolymerization and incomplete thermal cracking.

If a cable is operated at high temperature for a long time period then due to thermal oxidation a lot of hydroxyl group is generated. So, the polymeric chain of XLPE will break and it results in formation of multiple interfaces between spherulites and the amorphous region inside XLPE insulation [10-11].

2.3.2. CHEMICAL DEGRADATION:

Chemical degradation can affect physical properties of XLPE insulation. Chemical degradation leads to break up of long polymeric chains or formation of new cross-linking bridges. Chemically reactive free radicals are responsible for degradation process. These free radicals are formed during oxidation process inside the insulation. The formation rate of these free radicals is depended upon temperature, moisture content, presence of O_2 gas, radiation. Partial discharges inside the insulation lead to ionising radiation results formation of free radicals. As a consequence of partial discharges, some harmful gases are also formed. Sunlight contains UV radiation, which can affect polymeric insulation [12].

2.3.3.ELECTRICAL DEGRADATION:

Electrical degradation process is the most dangerous and it can cause serious damage to polymeric insulation. Water tree, electrical tree and partial discharge are the most important mechanism of electrical degradation. Electrical degradation is a random process and it affects insulation locally. Electrical degradation doesn't affect the whole length of cable, as thermal degradation does. Breakdown due to electrical degradation are associated with a specified region.

2.3.4.WATER TREEING:

XLPE cables are generally installed undergrounded are exposed to moisture and as a result, are prone to degradation due to water trees. Water tree normally initiates and propagates through cable insulation in presence of high intensity alternating electric field. Initiation and growth of water tree mainly depend on impurity content and micro-voids inside the insulation. Water can penetrate inside the cable insulation in the absence of water blocking barrier outside the cable. Defective joints or termination point are the points through which water can penetrate inside the insulation. Formation of water tree is a microscopic inhomogeneous process. Moisture content present inside insulation propagates in the path of the applied electric field in form a tree-shaped structure. Depending on formation and shape water tree can be divided into 2 types, bow-tie water tree and vented water tree. Bow-tie type water tree initiates from impurities and micro-voids present inside the insulation. It can grow in both direction and the maximum length of these types of water trees are within 10 μm. These types of water tree do not affect insulation significantly at low electric stress [12]. Residual moisture content from cross-linking can lead to bow-tie water tree but it is not considered to be dangerous. Vented water tree is originated from the interfaces between semiconducting parts and insulation and propagates in the direction of electric field. Initiation of vented water tree is slower than the bow-tie water tree. Bow-tie type water tree saturates after a certain length whereas vented water tree can penetrate through entire insulation. Vented water tree is thus more detrimental than bow-tie water tree. Initiation of a water tree may lead to localised degradation due to stress intensification [13-14]. Alternatively, significant oxidation may result due to water tree at high temperature, leads to increased absorption, higher conductivity, and eventually thermal runaway [8]. Water tree differs from an electrical tree in such a way that it doesn't form a prominent channel through the insulation. Water tree may disappear when alternating electric field and moisture content are removed.

Breakdown may occur when a branch of water tree bridges the electrodes. Though few cables can operate even after water tree bridges two electrodes. Growth of water tree is a very slow process, it takes several years. Initiation and formation of water tree depend on many factors like amplitude and frequency of applied alternating electric field, moisture content present inside insulation, quality of insulation [12,14].

2.3.5. ELECTRICAL TREEING AND PARTIAL DISCHARGE:

An Electrical tree is one of the primary causes of insulation failure in XLPE cable. A number of fine conductive channels propagate in the direction of the applied electric field to generate an electrical tree. Eroded surface due to micro-voids or water tree can cause stress intensification which may results initiation of electrical tree. Formation of an electrical tree can be divided into 2 phases i) initiation phase, ii) propagation phase. During the initiation phase at each half cycle of applied voltage some charge is trapped in the micro voids of the insulation which degrades the insulation gradually and leads to the formation of a comparatively larger void. Under the presence of a.c. electric stress polyethylene emits light in the visible and UV ranges above a certain threshold voltage due to the trapped charge. This UV light can cause photochemical reaction to generate free radicals which can break polymeric chain & bond leading to expansion of voids. During the propagation phase, a tree-shaped channel is formed due to partial discharge of the voids. Discharges above 5 pC are enough to cause thermal runaway and extensive local thermal degradation of the polymeric insulation. Initiation and propagation rate of an electrical tree depends on the amplitude and frequency of applied electrical stress, temperature, presence of voids [6]. Care has been taken during manufacturing though some impurities still remain inside the insulation in form of cavity or bubble which leads to partial discharge when applied voltage reaches above a threshold value. Partial discharge generates a number of positive ions and free electrons, which collide with other molecules to form electron avalanche which initiates degradation of the insulation. The degradation process will be in the form of conducting channels known as electrical tree. Total breakdown will occur when the conducting channel bridges 2 electrodes.

2.4. DIAGNOSTICS METHOD:

Main purposes of the diagnostics methods are to monitor the actual status of the insulation or to identify changes in the insulation structure or condition. Diagnostics methods of insulation involve both destructive and non-destructive ways [12]. Diagnostics methods also can be categorised in terms of whether they can be used on-site or not.

Generally, all diagnostics methods used on insulation systems on site should be non-destructive. The non-destructive methods are a common process as it does not involve shutting down and dismantling of the electrical equipment. Table 2.1 shows the diagnostics method used in underground cable insulation.

Table 2.1 Diagnostics method of power cable [12]

Diagnostics method	Insulation	Indicator	Description
Polarization Depolarization current measurement (PDC)	Oil-Paper, XLPE	Aging, Water trees, Moisture content	Off-line, on-site, non destructive
Frequency Domain Spectroscopy (FDS)	Oil-Paper, XLPE	Aging, Water trees, Moisture content	Off-line, on-site, non destructive
Frequency domain infrared spectroscopy (FTIR)	XLPE, Oil-paper	Moisture, chemical Changes	Off-line, off-site, destructive
Partial discharge measurement	XLPE	Aging, Voltage withstand	Off-line, on-site, destructive
Needle testing	XLPE	Voltage withstand	Off-line, off-site, destructive
Breakdown testing	XLPE, Oil-paper	Voltage withstand	Off-line, off-site, destructive
Tensile strength and elongation	XLPE	Material strength and stiffness	Off-line, off-site, destructive

CHAPTER-3

THEORY OF DIELECTRIC RESPONSE ANALYSIS

CHAPTER-3

3.1.INTRODUCTION:

In recent years overhead lines are replaced by underground cable in transmission and distribution system due to its excellent advantages. Underground cables have several unique benefits like lower transmission losses, can absorb emergency power loads, emits a lower magnetic field than overhead line etc. Underground power cables are used for bulk power transmission nowadays so, they play a key role in providing the reliable and efficient power supply. Operating underground for several years, the condition of cable insulation may deteriorate under a combination of "thermal, electrical, mechanical, chemical and environmental stresses". These stresses lead to physical, chemical degradation of the insulation which can be termed as "aging". Diagnostic tests are aimed to detect any kind of reduction in the physical strength of insulation due to the degradation processes. Physical, electrical and chemical degradation are the major degradation process affect the polymeric chain of cable insulation. This degradation causes structural changes, which generally increase the polarisation intensity and conductivity inside the cable insulation. A change in chemical or physical structure normally increases the dielectric losses. Many methods are employed for the diagnosis of the structural changes inside the insulation. Based on measured or derived parameters through these tests, some useful information about different stages of degradation as well as the root cause of degradation inside the insulation can be extracted. Over the past few years, several non-destructive diagnostics methods have been developed and employed. Dielectric response measurement is one of the popular tools for condition-based monitoring of XLPE cable, based on the fact that increased temperature, moisture content and water treeing can cause quantitive changes in the dielectric properties of insulation material [14-17]. Based on the theory of dielectric polarization there are 3 modern tools for dielectric response analysis 1) PDC (Polarization Depolarization Current measurement) 2) FDS (Frequency Domain Spectroscopy) 3) RVM (Recovery Voltage measurement) [17-20]. RVM method is not so popular for XLPE cable insulation as it is affected by the length for long cable [20].

3.2.DIELECTRIC RESPONSE MEASUREMENT METHOD:

The dielectric response of an insulation system can be measured either in the time domain or the frequency domain. PDC & RVM are time domain method whereas FDS is a

frequency domain method. In the thesis PDC is applied for time domain analysis & FDS is used for frequency domain analysis.

3.3.TIME DOMAIN SPECTROSCOPY:

Dielectric response in time domain can be analyzed by means of polarization and depolarization current.

When a dielectric material is subjected to an electric field, a relative shift between positive and negative charge takes place which leads to dielectric polarization [21]. There are 4 kinds of polarization mechanism 1) "Electronic Polarization" 2) "Ionic Polarization" 3) "Orientational Polarization" 4) "Interfacial Polarization". Out of these, Interfacial and Orientational polarization mechanism are a slow process and active in power frequency or even lower frequency range [21-22].

For a vacuum insulated system, electric flux density "D" is directly proportional to applied electric field "E", given by

$$D = \varepsilon_0 E \tag{3.1}$$

If the vacuum is replaced by homogenous dielectric medium then polarization should be considered, so equation 3.1 can be written as,

$$D = \varepsilon_0 E + P \tag{3.2}$$

If the applied electric field is time varying in nature, then equation (3.2) can be written as,

$$D(t) = \varepsilon_0 E(t) + P(t) \tag{3.3}$$

Where *P(t)*is defined as,

$$P(t) = \chi(t)\varepsilon_0 E(t) \tag{3.4}$$

χ= electrical susceptibility of dielectric material.

So, from the equation (3.3) & (3.4) *D(t)* can be expressed as,

$$D(t) = \varepsilon_0(1+\chi(t))E(t) \tag{3.5}$$

The polarization vector, *P*(t) combination of all polarization mechanism in a dielectric material. As, polarization process has large settling time, hence at $t \rightarrow \infty$, $P(t)=P_S$. If a step voltage source U_0 is applied, then the polarization vector *P*(t) maintain exponentially increasing profile. So, polarization vector can be simplified as,

$$P(t) = (P_s - P_\infty) g(t - t_0) + P_\infty \delta(t - t_0) \tag{3.6}$$

Where $\delta(t-t_0)$ is delta function, very fast polarization process occurring within a very short time period & its magnitude is very large. $g(t-t_0)$, exponentially increasing function with time, reflects the slow polarization process (interfacial, dipolar).

Where,

$$\begin{aligned} g(t - t_0) &\geq 0 \quad for \quad t_0 < t < \infty \\ g(t - t_0) &= 0 \quad for \quad t = t_0 \\ g(t - t_0) &= 1 \quad at \quad t \rightarrow \infty \end{aligned}$$

Using equation (3.4) & (3.6) polarization vector *P(t)* can be written as,

$$P(t) = [\chi_\infty + (\chi_s - \chi_\infty) g(t - t_0)] \varepsilon_0 E(t) \tag{3.7}$$

Susceptibility can be related with permittivity of the dielectric medium as, $\varepsilon=1+\chi$. Therefore, equation (3.7) can be expressed as,

$$P(t) = [\varepsilon_\infty + (\varepsilon_s - \varepsilon_\infty) g(t - t_0)] \varepsilon_0 E(t) \tag{3.8}$$

Dielectric material cannot polarize instantly after the application of electric field *E(t).* Polarization function is a convolution of the electric field at previous times with time-dependent susceptibility. So, *P*(*t)* can be expressed by,

$$P(t) = \varepsilon_0 (\varepsilon_\infty - 1) E(t) + \varepsilon_0 \int_{-\infty}^{t} f(t - \tau) E(\tau) d\tau \tag{3.9}$$

Where *f(t)* is a dielectric response function which reflects the polarization process in a dielectric and can be expressed by,

$$f(t) = (\varepsilon_s - \varepsilon_\infty) \frac{dg(t)}{dt} = (\chi_s - \chi_\infty) \frac{dg(t)}{dt} \tag{3.10}$$

Therefore, under the presence of applied electric field *E(t)* displacement current density *J(t),* can be written as based on the Maxwell equation,

$$J(t) = \sigma_0 E(t) + \frac{\partial D(t)}{\partial t} = \sigma_0 E(t) + \varepsilon_0 \frac{\partial E(t)}{\partial t} + \frac{\partial P(t)}{\partial t} \tag{3.11}$$

Where σ_0= d.c. conductivity of the sample.

Using equation and taking *E(t)*=constant,

$$J(t) = \sigma_0 E(t) + \varepsilon_0(\varepsilon_\infty \delta(t) + f(t))E(t) \tag{3.12}$$

For a homogeneous dielectric total current through the dielectric can be express as,

$$i(t) = C_0 U_0[\frac{\sigma_0}{\varepsilon_0} + \varepsilon_\infty + f(t)] \tag{3.13}$$

Where C_0 = geometric capacitance of the sample. As seen in equation (1), current *i(t)* has 3 parts first part is conduction current which reflects d.c. conductivity of the sample and is independent of any kind of polarization process. Second part or delta function cannot be recorded due to fast polarization process occurring within a very short time period & its magnitude is very large. Third part *f(t)* defines all kind of active polarization process in the sample.

3.3.1. POLARIZATION DEPOLARIZATION CURRENT MEASUREMENT:

Polarization depolarization current measurement or PDC is one of the popular methods for time domain dielectric response analysis. In this method, a step voltage source is applied to the sample to investigate the polarization process in a dielectric. Before the PDC experiment dielectric memory of the sample should be cleared [22]. The system should be isolated or shielded during the PDC experiment to avoid noise and better accuracy.

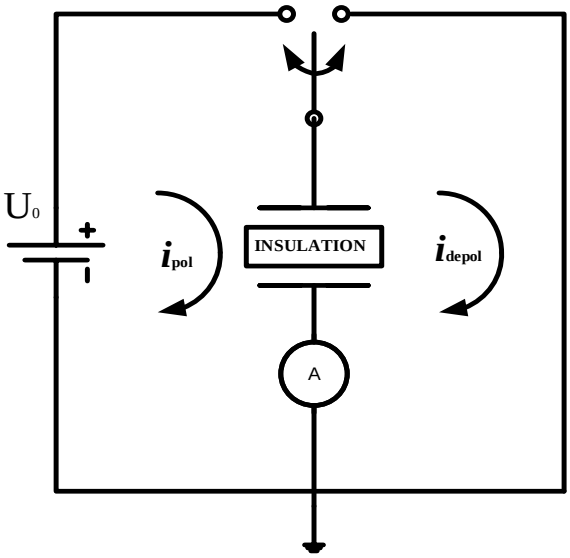

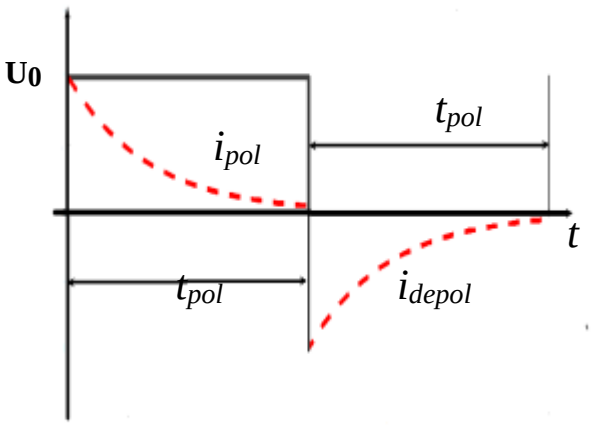

Fig.3.1. Circuit diagram of PDC measurement [22] ***Fig.3.2. Polarization depolarization current nature [22]***

Fig. 3.1 shows basic PDC measurement circuit diagram. This measurement process includes applying a step voltage source U_0 on the dielectric sample for a large time span 0

$\leq t \leq t_{pol}$ in order to initiate the polarization process. The current during this time span can be termed as charging current or polarization current (i_{pol}). It can be expressed as,

$$i_{pol} = C_0 U_0 [\frac{\sigma_0}{\varepsilon_0} + \varepsilon_\infty \delta(t) + f(t)] \quad (3.14)$$

If charging time span (t_{pol}) is very large in order of 1000s- 10000s, then polarization current becomes steady and only conduction current flows. If the applied voltage is removed and the sample is shorted at $t=(t_{pol})$, then the sample starts to discharge and the current recorded is termed as depolarization or discharging current (i_{depol}). Depolarization current is also termed as Isothermal current if the temperature remains constant during depolarization process. Where,

$$i_{depol} = -C_0 U_0 [\varepsilon_\infty \delta(t) + \{f(t) - f(t + t_{pol})\}] \quad (3.15)$$

δ(t) is a very short duration current of large amplitude, so it can be neglected. If the sample is charged for a long duration $0 \leq t \leq t_{pol}$ then the term $f(t + t_{pol})$ in the equation (3.15) can be neglected. Hence, equation (3.15) can be expressed as,

$$i_{depol} \approx -C_0 U_0 \{f(t)\} \quad (3.16)$$

According to equation (3.16) depolarization current is controlled exclusively by the dielectric response function $f(t)$ with time. Therefore, it is easy to draw some simple conclusions from its magnitude. Voltage profile and nature of polarization current and depolarization current during PDC measurement is shown in Fig.3.2 where t_{pol} and t_{depol} denote polarization and depolarization time respectively. Both polarization current (i_{pol}) and depolarization current (i_{depol}) depend upon the geometry and physical properties of the insulation system [23-25].

3.3.2. ***PDC MEASUREMENT FLOWCHART [22]:***

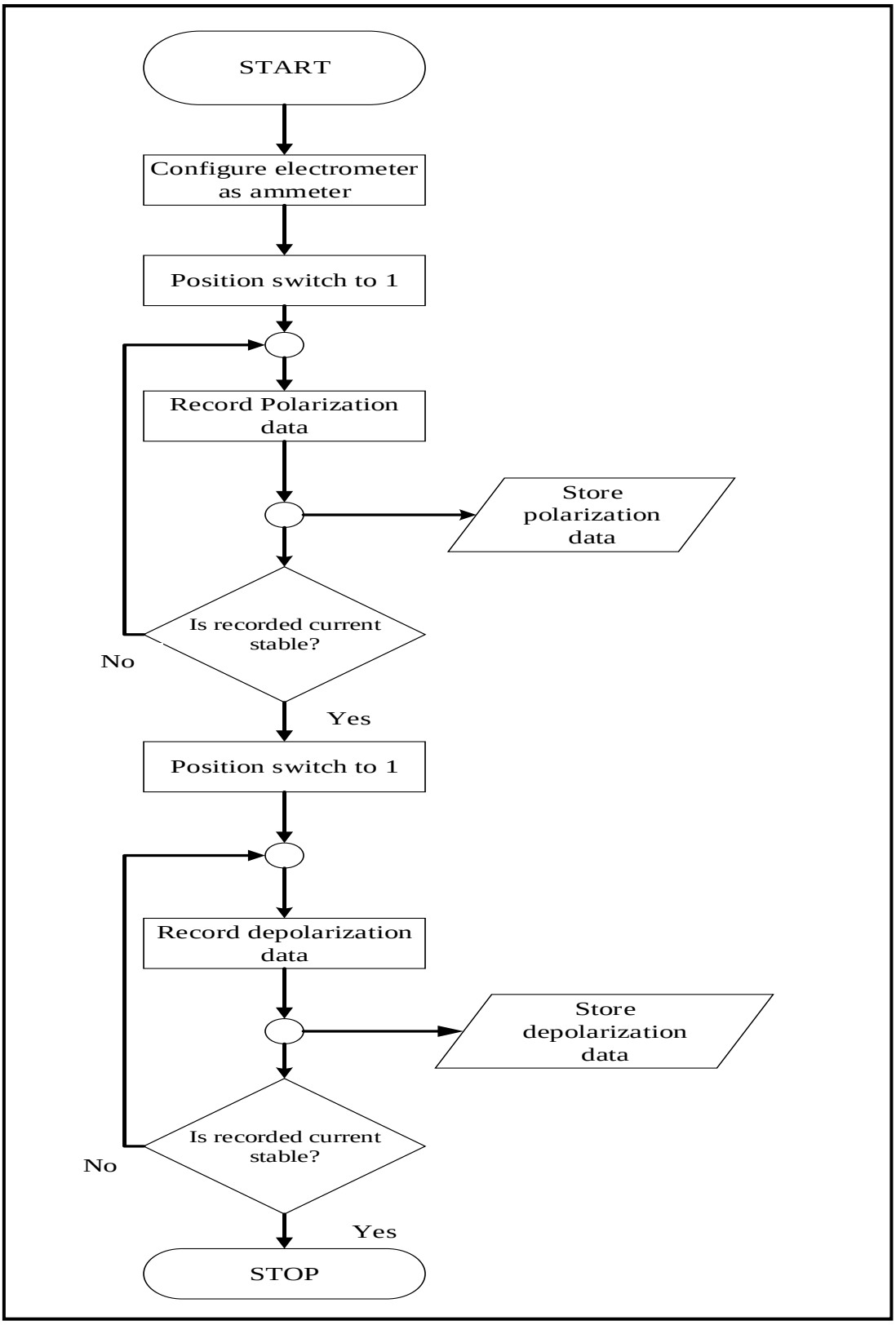

Fig. 3.3 PDC measurement flowchart

3.3.3.ADVANTAGES OF PDC MEASUREMENT:

- PDC is a non-destructive tool for condition monitoring and it can provide an idea about polarization spectra in a sample.
- Conductivity, time-varying relaxation processes of a dielectric can be analyzed by PDC data.
- It can provide a very fast response at low-frequency with good accuracy.

3.3.4.LIMITATIONS OF PDC MEASUREMENT:

- The magnitude of polarization and depolarization current is very small in the range of (nA-pA), so measurement can be affected due to external noise.
- Due to high noise sensitivity proper shielding prior to experiment is very much important.
- High voltage source is required for PDC measurement for better accuracy.

3.4.FREQUENCY DOMAIN SPECTROSCOPY:

Though PDC measurement is widely used for condition monitoring of XLPE insulation but it has a certain limitation. The main disadvantages of PDC measurement are, i) a high voltage source is required for measurement purposes and ii) it is susceptible to noise. So researchers have been considering FDS as a better method for monitoring the condition of a solid insulation system like XLPE. In this method, a sinusoidal voltage is applied and the dissipation factor or tan delta is measured as a function of frequency [19, 21]. Measurement in the frequency domain requires a sinusoidal voltage source of variable frequency. A basic circuit diagram of FDS measurement has been shown in Fig.3.4.

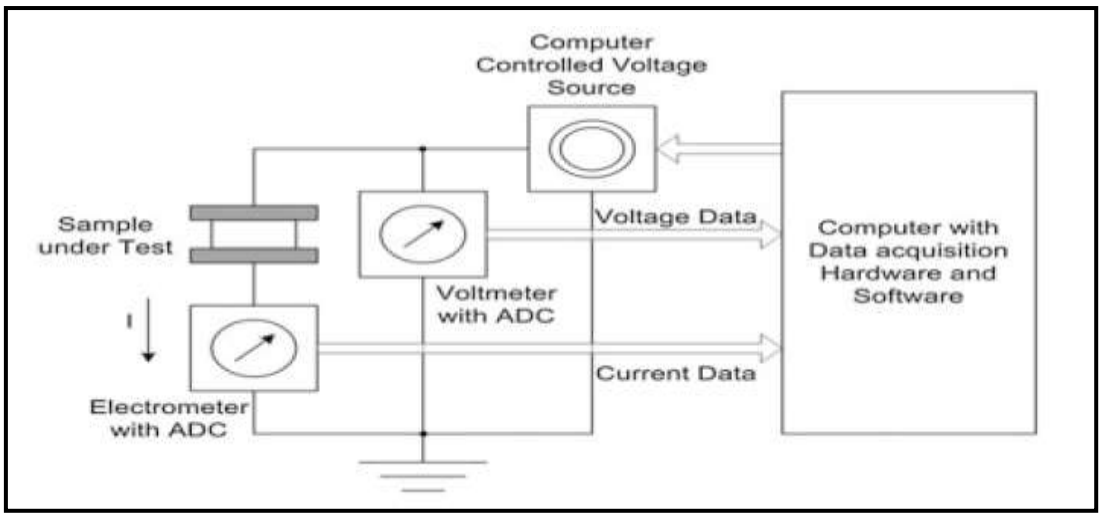

Fig. 3.4. FDS measurement circuit diagram [22]

In the frequency domain analysis, a pure sinusoidal voltage $U_0(\omega)$ is applied on the insulation. Under the presence of sinusoidal electric field, polarization process begins and dielectric response current flows through insulation. Using Fourier transformation equation (3.14) can be written as,

$$I_m(\omega) = C_0 U_0[\frac{\sigma_0}{\varepsilon_0} + j\omega\varepsilon_\infty + j\omega F(\omega)] \tag{3.17}$$

$F(\omega)$ = Fourier transform of a dielectric function $f(t)$ where $F(\omega)$ can be related to the susceptibility of the dielectric sample as,

$$F(\omega) = \int_0^\infty f(t)\, e^{-j\omega t} dt = \hat{\chi}(\omega) = \chi'(\omega) - j\chi''(\omega) \tag{3.18}$$

$\hat{\chi}(\omega)$ = complex susceptibility of the sample, where $\chi'(\omega)$ = real part of the complex susceptibility and $\chi''(\omega)$ = imaginary part of the complex susceptibility.

Based on equation (3.18), equation (3.17) can be expressed as,

$$I_m(\omega) = j\omega C_0[1 + \chi'(\omega) - j(\frac{\sigma_0}{\varepsilon_0\omega} + \chi''(\omega))]U_0(\omega) \tag{3.19}$$

$$\text{or, } I_m(\omega) = j\omega C_0[\varepsilon'_r(\omega) - j\varepsilon''_r(\omega)]U_0(\omega) \tag{3.20}$$

$$\text{or, } I_m(\omega) = j\omega[C'(\omega) - C''(\omega)]U_0(\omega) = j\omega\hat{C}(\omega)U_0(\omega) \tag{3.21}$$

Often it is more suitable to use complex permittivity instead of complex susceptibility can be expressed as $\varepsilon'_r(\omega) - j\varepsilon''_r(\omega)$.

Complex susceptibility $\hat{\chi}(\omega)$ can be related to the complex permittivity $\hat{\varepsilon}(\omega)$ through the following equation,

$$\varepsilon'_r(\omega) = 1 + \chi'(\omega) \tag{3.22}$$

$$\varepsilon''_r(\omega) = \frac{\sigma_0}{\varepsilon_0\omega} + \chi''(\omega) \tag{3.23}$$

$\hat{C}(\omega)$ is the frequency dependent complex capacitance of the dielectric sample. The real part of complex capacitance $C'(\omega)$ reflects the energy storage capacity of a dielectric during the polarization process. Imaginary part of the complex capacitance, $C''(\omega)$ of an insulating material emblematizes the lossy nature of the dielectric material. Under the

application of alternating electric field absorption of electrical energy by the dielectric material can be termed as “dielectric loss”. Dielectric losses in a dielectric material under the presence of alternating electric filed are mainly owing to the d.c. conductivity of the dielectric material and friction losses between different dipoles. Losses due to the d.c. conductivity is becoming predominant under the presence of low-frequency sinusoidal voltage, where the time period of one-half cycle is large enough to cause long-range charge migration [26]. Frictional losses between the dipoles are mainly owing to all kinds of active polarization process inside the dielectric material.

Dissipation factor or tanδ is defined as the ratio of heat loss to the energy storage in a dielectric medium, can be represented as,

$$\tan\delta(\omega) = \frac{C''(\omega)}{C'(\omega)} = \frac{\frac{\sigma_0}{\varepsilon_0\omega} + \chi''(\omega)}{\varepsilon'_r(\omega)} \tag{3.24}$$

Measurement of tanδ for assessing the condition of insulation is preferable from a practical point of view because it is independent of the geometry of the test object, and should not depend on the applied voltage [19]. According to equation (3.24) tanδ is a function of the frequency of applied sinusoidal voltage.

3.4.1.<u>ADVANTAGES OF FDS MEASUREMENT:</u>

- Frequency domain spectroscopy (FDS) provides information about frequency-dependent heat dissipation factor and the real and imaginary part of the complex capacitance.
- It is a non-destructive method and provides information about moisture content or migrated water content inside a solid insulation.
- FDS has better noise performance.
- FDS provides an idea about the characteristics of polarizability (χ') and losses (χ'') in a dielectric medium.

CHAPTER-4

EXPERIMENTAL STUDY

CHAPTER-4

4.1.INTRODUCTION:

Failure of the insulation system of the underground power cable is very much undesirable nowadays. Regular condition monitoring of power cable has thus gained popularity to extend the longevity of the insulation system. This will increase the reliability of the underground transmission and distribution system.

As described in the section (2.4) there are two methods of condition monitoring 1) destructive method, 2) non-destructive method. Non-destructive methods are more popular in modern days because of the fact that we need not have to shut down the whole system for a long time period. Dielectric response measurement is one of those preventive diagnostic tools used for condition monitoring of XLPE cable insulation.

This chapter describes the sample preparation, experimental procedure and the experimental results in details.

4.2.SPECIFICATIONS OF CABLE:

1-core XLPE cable has been chosen for the experiment and the specifications of the cable are here as follows,

Table 4.2. Specifications of cable

Property	Cable
Type	1-core
Insulation	XLPE
Length (cm)	27
Rated Voltage (kV)	11
Insulation Thickness (mm)	3.4
Relative permittivity	2.25
Area of conductor (mm^2)	240
Manufacturing Company	KEC

4.3.SAMPLE PREPARATION USING XLPE CABLE:

This section chronicles the preparation of the samples in a certain way prior to the experiment. For this experiment, only copper tape, semiconductor layer, XLPE insulation and core of the cable is used.

In High tension laboratory of Jadavpur University, firstly 1-core XLPE cable samples were collected and cut into a suitable dimension to measure the dielectric response. On the both end of the sample, the conductor part was exposed by removing the insulation part. The outer sheath and copper tape of 5 cm was removed and the outer semiconductor layer of 3 cm was also peeled off leaving behind the XLPE insulation over the conductors in the one end of the sample. Actual photograph of the 1-core XLPE cable prepared for the experiment has been shown in Fig. 4.1

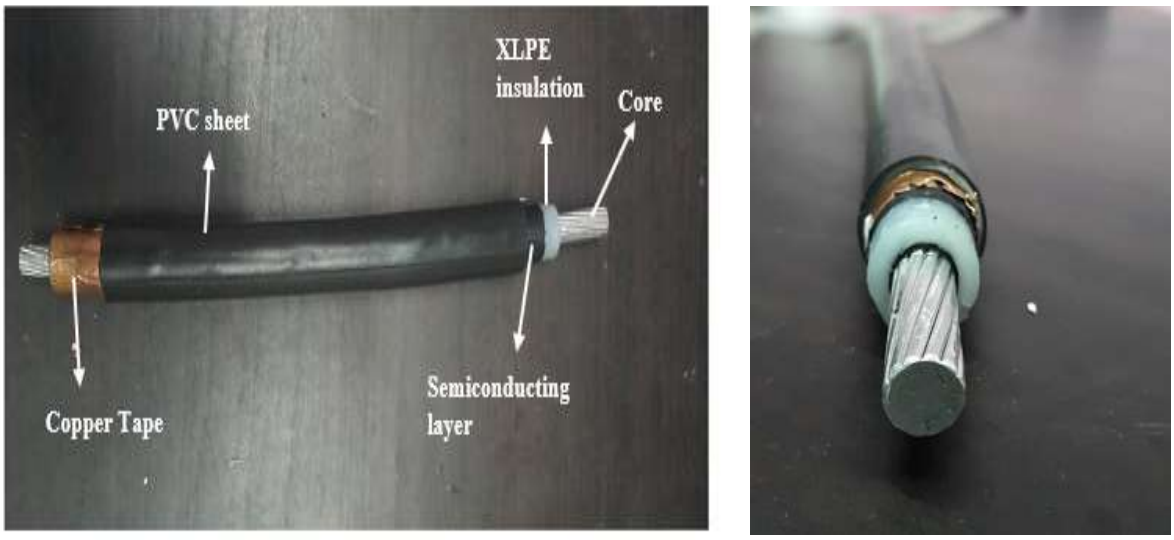

Fig.4.1. Photograph of 1-core XLPE cable sample prepared for experiment (a) top view of the sample under test (b) Side view of the sample

4.4.EQUIPMENTS EMPLOYED:

Several types of equipment were employed during the experimental process. High Tension Laboratory of Jadavpur University provides a wide range of equipment and instruments for dielectric response analysis of XLPE cable. Detail information of these equipment has been elaborated as follows.

4.4.1.THERMAL OVEN:

The thermal oven, as shown in figure 5.7, maintains a controlled temperature in an isolated chamber by means of a thermostat. The temperature range of this oven is 25°C-90°C.

Therefore, XLPE cable has been placed in a thermal oven to control the operating temperature in the present work.

Fig 4.2 Thermal oven

4.4.2.THE DIRANA:

DIRANA or dielectric response analyser is used to monitor the condition of high voltage insulation systems like in power transformer, cable, generator and bushing through dielectric response analysis. The one through which experiments were carried out bears the model number VEHP0072 manufactured by OMCORN. In the present work, it was used for Polarization Depolarization Current (PDC) measurement. It can measure polarization depolarization current up to 10000sec. It is also used for frequency domain measurement. Photograph of the DIRANA and its accessories has been shown in Fig.4.3.

Fig. 4.3. DIRANA and its accessories

4.4.3.THE IDAX:

IDAX or Insulation Diagnostic Analyzer is used to investigate insulation condition based on frequency domain spectroscopy. The model number of the device through which experiments were carried out is IDAX-300. It can measure the dissipation factor in the frequency range 40000Hz-0.1mHz. Photograph of the IDAX-300 has been shown in Fig.4.4.

Fig. 4.4. IDAX-300

4.4.4.LCR METER:

An LCR meter is a type of electronic device used to measure the inductance (L), capacitance (C), and resistance (R) of a test object. Model no of the LCR meter is HTC-F3. In the present work, LCR meter is used to measure the capacitance of XLPE cable insulation. Picture of an LCR meter has been shown in Fig. 4.5.

Fig.4.5. LCR meter

4.5.EXPERIMENTAL PROCEDURE:

After the completion of sample preparation, dielectric response tests namely Time domain spectroscopy (TDS) and Frequency domain spectroscopy (FDS) were carried out. During the experiment, high voltage electrode was connected to the conductor part and the measuring electrode was connected to the copper tape of cable to provide a return path. Peeled off XLPE insulation was grounded through a copper wire to prevent leakage current from the surface of the insulation. Dielectric response measurement was performed on the cable at 5 different temperature i.e. 25°C, 40°C, 50°C, 60°C and 70°C. Prior to experiment cable was placed in a thermal oven, where it was heated for at least 3 hours at the aforementioned temperatures.

As discussed in the section 2.3.4, water tree degradation is one of the primary causes of insulation failure in XLPE cable. To simulate water tree inside XLPE insulation, contaminated water was injected inside the insulation by creating an artificial defect on the insulation surface. Since the dimension of water tree is in the range of μm, so total accumulated water inside a cable insulation due to water treeing can be correlated with the injected water inside the insulation by creating artificial holes. For artificial defect in XLPE insulation uniform holes (depth of 2.8mm, diameter of 0.5mm) were drilled on the insulation surface using an electric drill. Photograph of the drilled hole on the insulation surface has been shown in Fig.4.6. NaCl (0.1mol/L) was mixed with water to produce contaminated water solution. Then this contaminated water was injected into the holes. For water content variation inside the insulation more no of holes were drilled on the insulation surface.

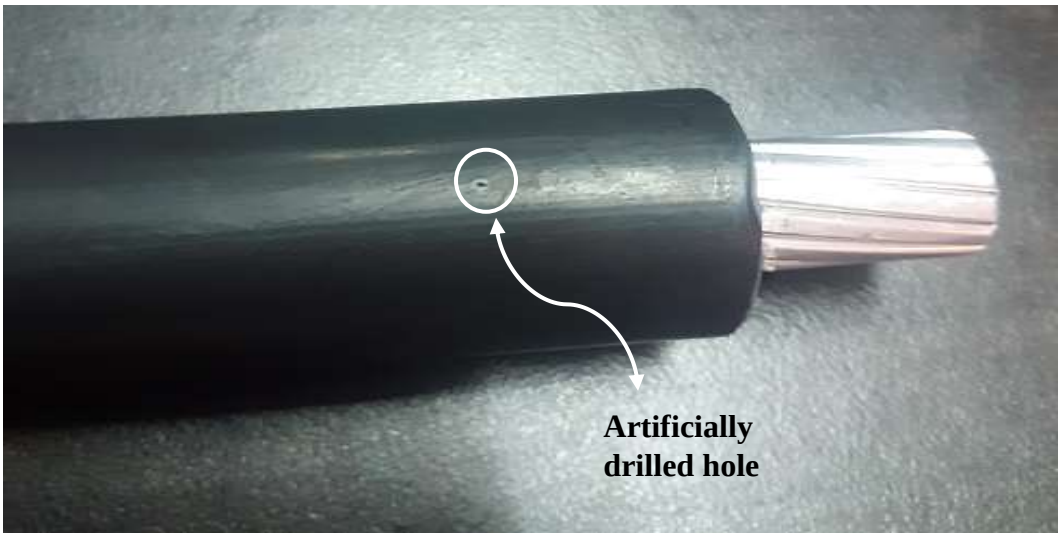

Fig. 4.6. Artificial defect created on XLPE insulation surface

The water present inside the cable insulation is quantified as water content. Water content in a solid can be divided into gravimetric and volumetric water content. In this thesis volumetric water content or VWC was chose to quantify the water present inside the insulation. It can be defined as the ratio of volume of injected water to the total volume insulation and denoted by "θ_w". It can be represented as parts per million or ppm. Where,

$$\theta_w(ppm) = \frac{V_w}{V_i} \times 10^6 \qquad (4.1)$$

V_w = Volume of injected water, V_i= volume of the insulation.

In this present work water content in the XLPE insulation was varied from 13 ppm to 78 ppm. Therefore, by performing dielectric response measurement on XLPE cable at different water content we can get an idea about different stages of water tree aging in XLPE cable insulation.

For PDC measurement, DIRANA manufactured by OMCRON was used. Applied voltage was set at 200V and polarization and depolarization time was set as 1000s. Here, the length of the cable is small so polarization time can be taken as 1000s. The schematic circuit diagram of PDC measurement has been shown in Fig.4.7. Since the magnitude of polarization depolarization current is very low in the range of nA-pA, so, it can be affected by external interference. Hence, the sample must be kept shielded during the experiment. In this experiment thermal oven was used as a shielded box.

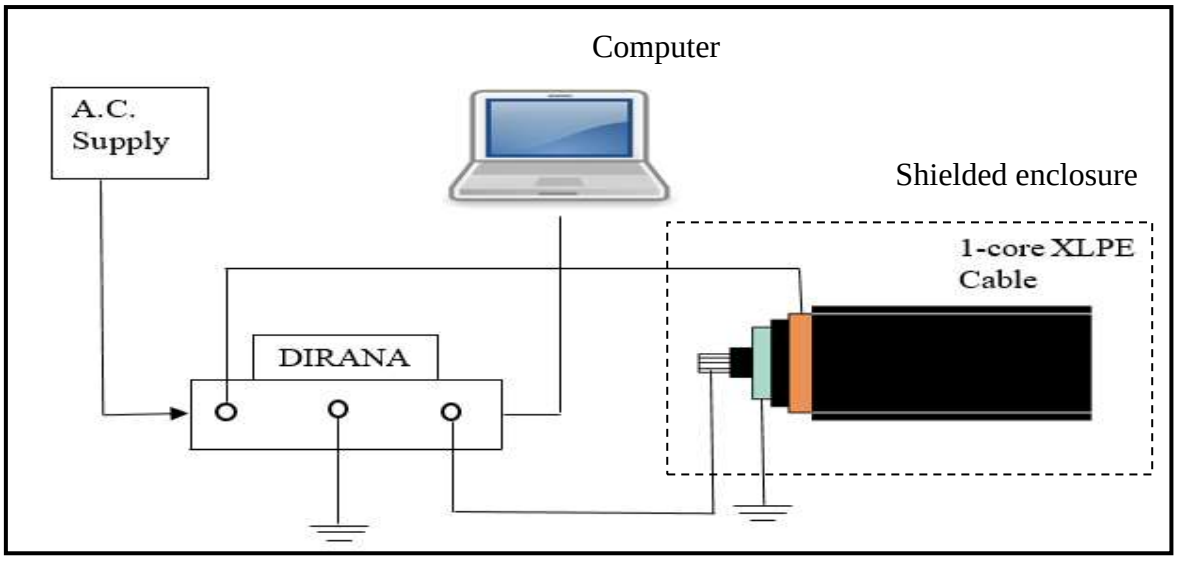

Fig.4.7. Schematic diagram of PDC measurement

In Fig.4.8 experimental setup for PDC measurement has been shown where cable is placed at thermal oven and connected to DIRANA.

Fig.4.8. Experimental setup for PDC measurement of XLPE cable using DIRANA

For Frequency domain measurement IDAX-300 manufactured by Megger was employed. Applied voltage was set at 141.4Vrms. The measurement frequency range is set at 1kHz – 0.2mHz. The Schematic diagram of FDS measurement is shown in Fig.4.9.

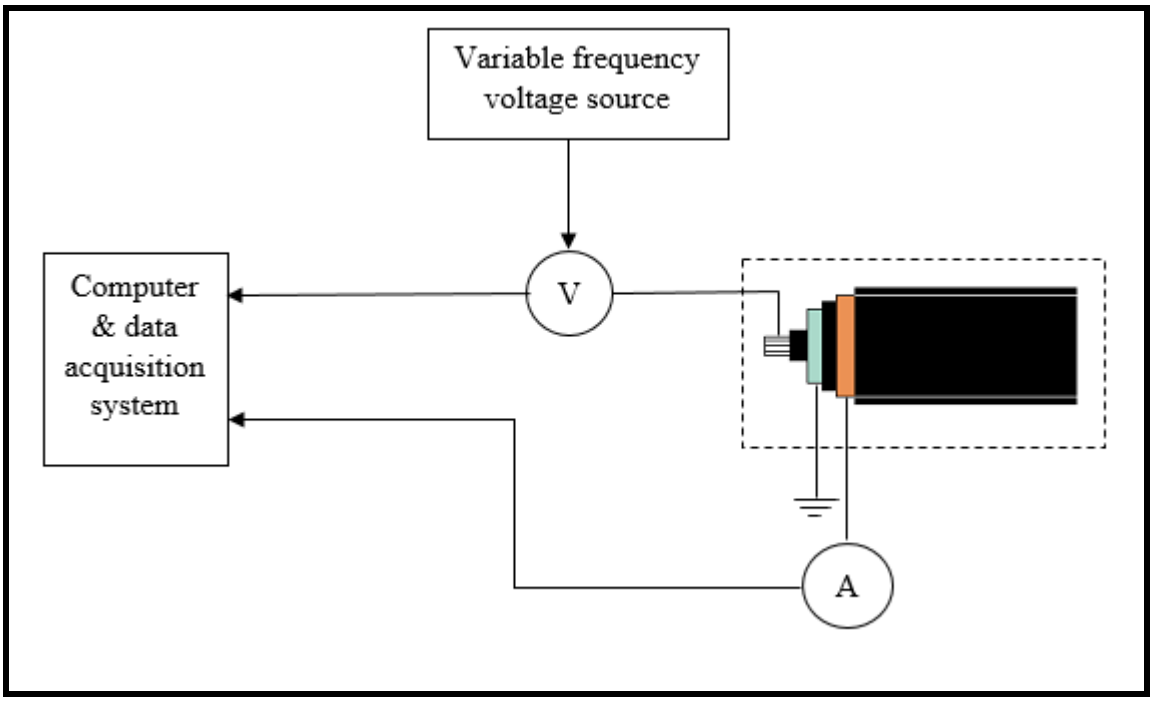

Fig .4.9. Schematic diagram of FDS measurement

Actual photograph of the experimental set up for FDS measurement is shown in Fig. 4.10 where the cable is placed at thermal oven and connected to IDAX-300.

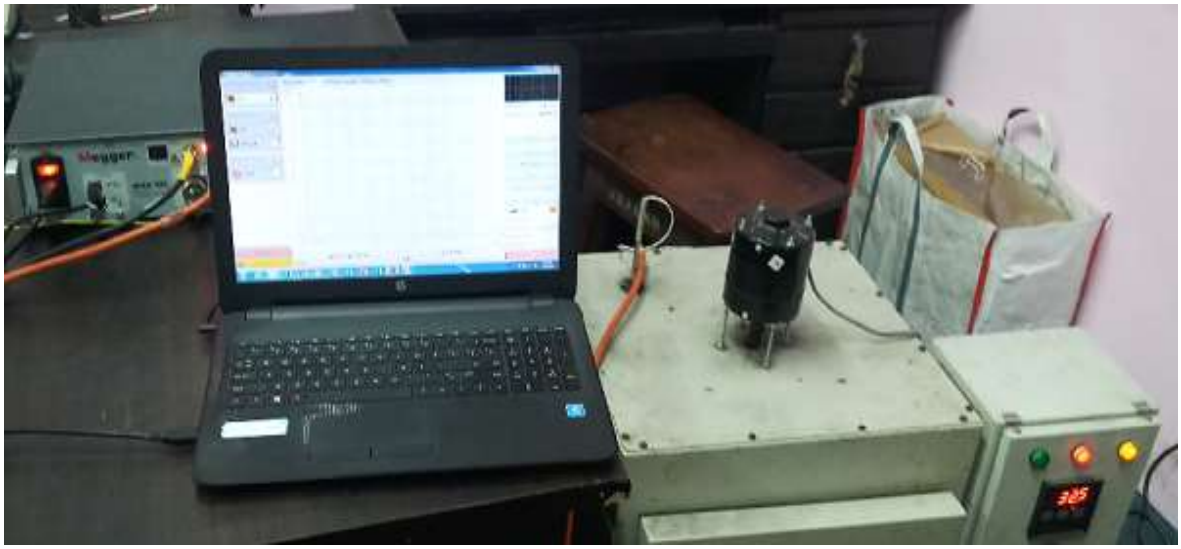

Fig.4.10. Experimental set up for FDS measurement of XLPE cable using IDAX-300

All the experiments and experiment related works were performed at High tension laboratory, Jadavpur University.

CHAPTER-5

RESULT AND DISCUSSION

CHAPTER-5

5.1.INTRODUCTION:

In the previous chapter different stages of sample preparation and experiment procedure has been discussed in detailed. Now, the results obtained are explored and discussed in this chapter and a comparative study based on the dielectric response parameters is performed on the basis of the data acquired. Firstly, the capacitance of the sample has been measured through LCR meter. The geometric capacitance of the sample can be calculated by dividing the measured capacitance with the relative permittivity of the sample. Then, for analyzing the dielectric polarization processes of the cable sample, dielectric spectroscopy measurements were performed on it. Dielectric spectroscopy measurements can be performed in both time domain and frequency domain. In the present work, the dielectric spectroscopy measurements were performed in both domains.

5.2.VALUE OF GEOMETRIC CAPACITANCE:

The geometric capacitance is defined as the vacuum capacitance of the electrode arrangement between which the dielectric is sandwiched or it can be also defined by the high- frequency capacitance of the dielectric at the time at which the current measurement was started [22]. It is denoted by C_0.

Measured value of capacitance of the XLPE cable sample under test is 68 pF. As dielectric constant of XLPE is 2.25 at 50 Hz [27], hence, the geometric capacitance (C_0) of the sample is 30.22 pF.

5.3.COMPARATIVE STUDY OF PDC MEASUREMENT:

As discussed in the earlier chapter, the Polarization-Depolarization Current (PDC) measurement incorporates application of a d.c. electric field on a dielectric specimen for a fixed time interval and subsequent removal of it. During this process, the charging or polarization current and discharging or depolarization current are recorded and analyzed. In the present work PDC experiments were performed on XLPE cable at different operating temperatures and at different water content inside the insulation. Polarization current curves of the XLPE cable sample at different operating temperatures and at different water content are displayed as follows.

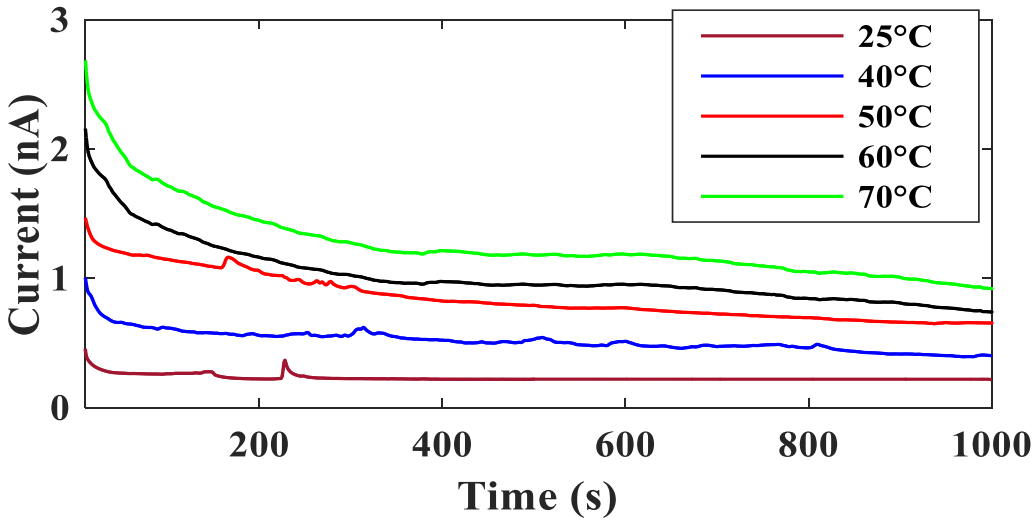

Fig 5.1 Polarization current curve for different operating temperature

Fig. 5.1 shows the polarization current of XLPE cable sample for 5 different operating temperatures i.e. 25°C, 40°C, 50°C, 60°C and 70°C. The time duration for the polarization current is 1000 sec and the applied d.c. voltage is 200 V.

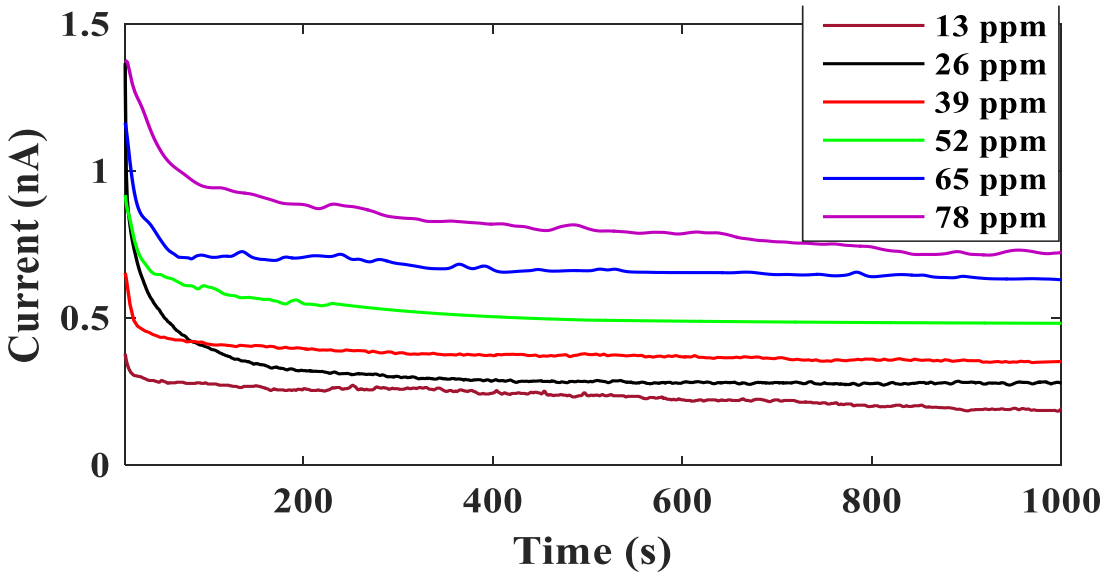

Fig 5.2 Polarization current curve for the variation of water content in XLPE cable insulation

Fig.5.2 shows the polarization current of XLPE cable sample for different water content inside the cable insulation. The time duration for the polarization current is 1000 sec and the applied d.c. voltage is 200 V.

Polarization current has 3 parts, as given in the equation (3.14), a stable part of the polarization curve is conduction current which depends upon the d.c. conductivity of the insulation (σ_0), remaining part emblematizes the polarization process inside the insulation, which decay's exponentially with time. Current due to delta function can't be recorded in

the polarization curve as it is due to fast polarization process. According to Fig 5.1 and 5.2, the magnitude of polarization current increases with the increment of temperature as well as the accretion of water content inside the insulation. In Fig. 5.1 and Fig. 5.2, it is clearly visible that there are some spikes in the polarization curve. This is due to external noise which can affect the measurement. As, initial part of the polarization and depolarization current is prone to noise, so first few seconds of the measurement are neglected.

Depolarization current curves for XLPE cable sample have been shown as follows,

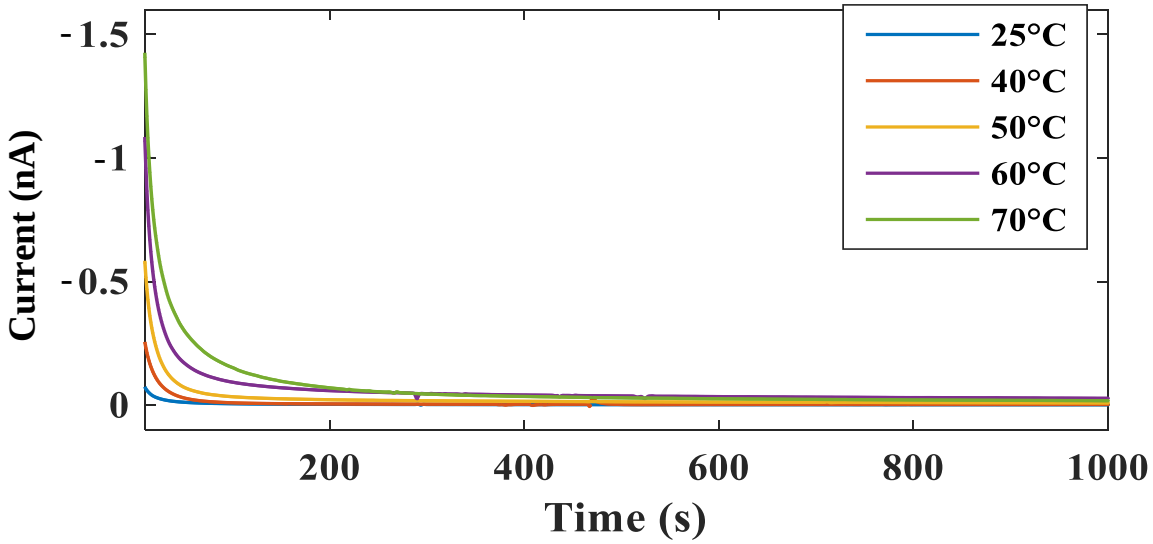

Fig 5.3 Depolarization current curve for different operating temperature

Fig. 5.3 shows the depolarization current of XLPE cable sample for 5 different operating temperatures i.e. 25°C, 40°C, 50°C, 60°C and 70°C. The time duration for the polarization current is 1000 sec.

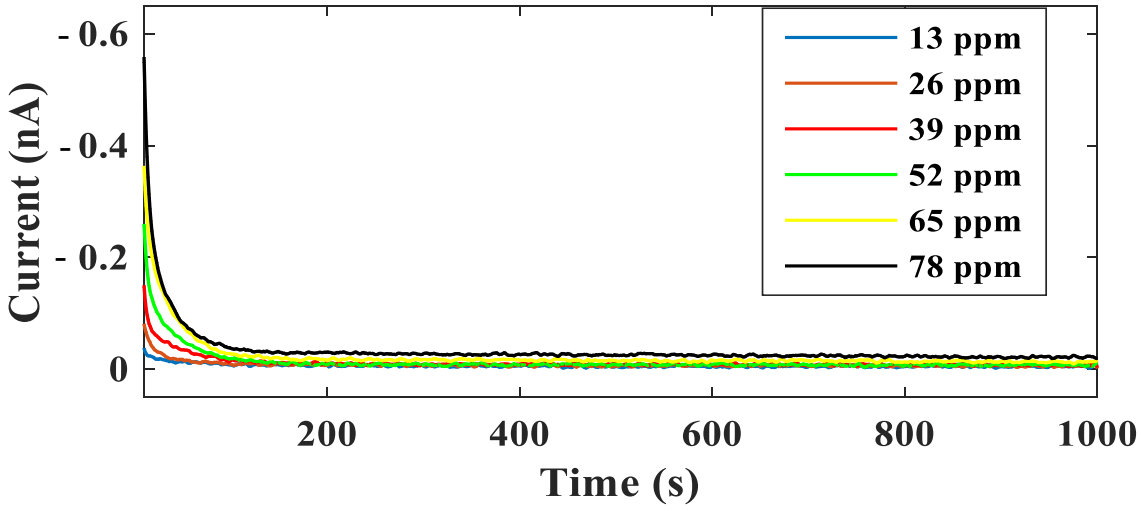

Fig 5.4 Depolarization current curve for variation of water content in XLPE cable insulation

Fig. 5.4 shows the depolarization current curves of XLPE cable sample for different water content inside the cable insulation. The time duration for the depolarization current is 1000 sec.

As discussed in the earlier chapter depolarization current is directly proportional to the active polarization process inside insulation. So, based on Fig 5.3 and Fig 5.4 it can be stated that the polarization process are increasing with the increment of operating temperature and water content. In the next chapter further analysis based on PDC curve has been shown.

5.4.COMPARATIVE STUDY OF FDS MEASUREMENT:

In frequency-domain measurement dissipation factor (tanδ) and real and imaginary capacitance of the insulation is measured. In the present work, the FDS experiment is performed at 5 different temperature and at 6 different water content inside cable insulation. Experimental results of the FDS experiment have been furnished as follows,

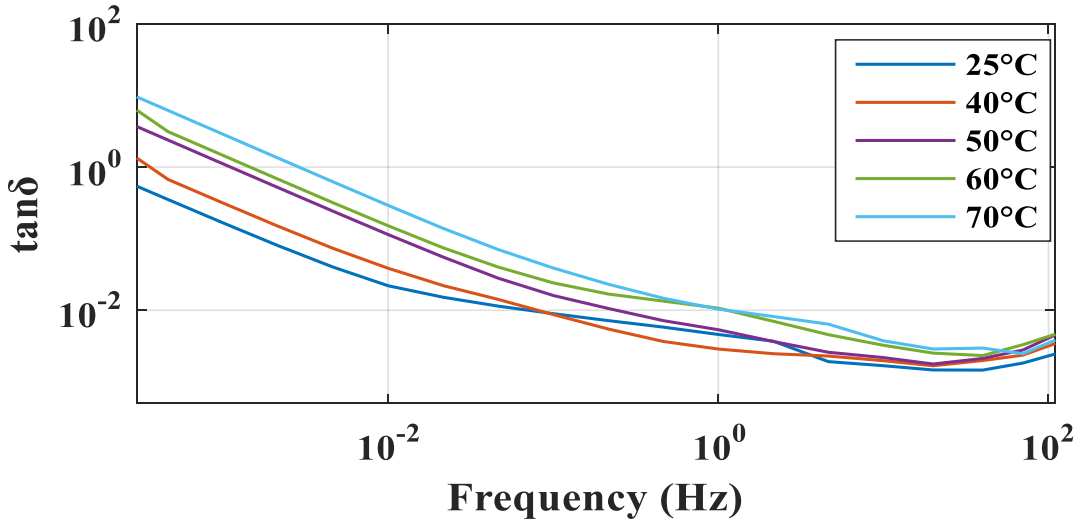

Fig 5.5 tanδ curve for different operating temperature

Fig. 5.5 shows the dissipation factor curve of XLPE cable sample with respect to frequency for different operating temperature. The frequency range of the curves is given as 0.2mHz -110Hz.

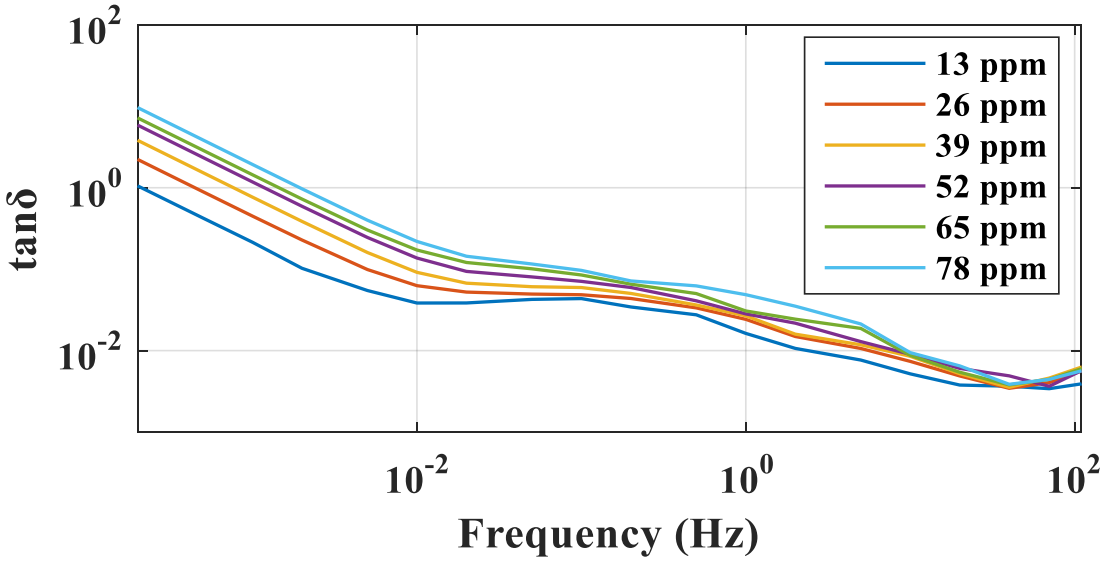

Fig 5.6 tanδ curve for different water content inside XLPE cable

Fig. 5.6 shows the dissipation factor curve of XLPE cable sample with respect to frequency for different water content inside the cable insulation. The frequency range of the curves is given as 0.2mHz -110Hz.

As given in equation 3.24, tanδ is inversely proportional to the frequency of applied voltage, therefore, from Fig. 5.5 & Fig. 5.6 it is clearly observed that the dissipation factor increases at a lower frequency region. In the higher frequency region, it is observed that tanδ increases with frequency. This can be explained as, under the application of high-frequency electric field frictional losses due to polarization process i.e. $\chi''(\omega)$ can increase. This may be the probable reason for the increment of tanδ in the higher frequency region.

Complex permittivity of a sample can be calculated by dividing complex capacitance measured through frequency domain spectroscopy, to the geometric capacitance (C_0) of the sample. Characteristics of the real part of complex permittivity $\varepsilon'_r(\omega)$ and imaginary part of complex permittivity $\varepsilon''_r(\omega)$ of XLPE cable at different operating temperature have been shown in Fig. 5.7 (a) & Fig. 5.7 (b) accordingly,

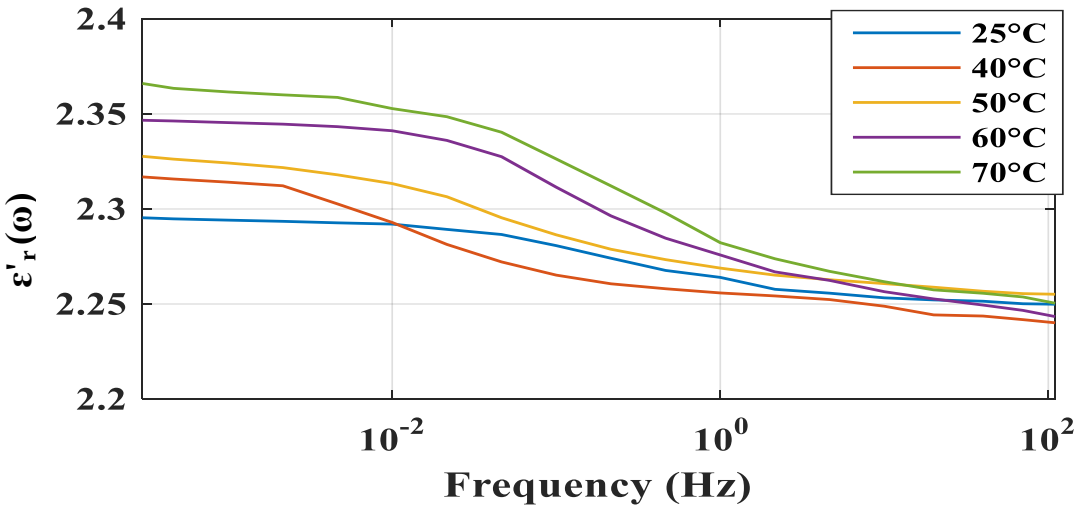

(a)

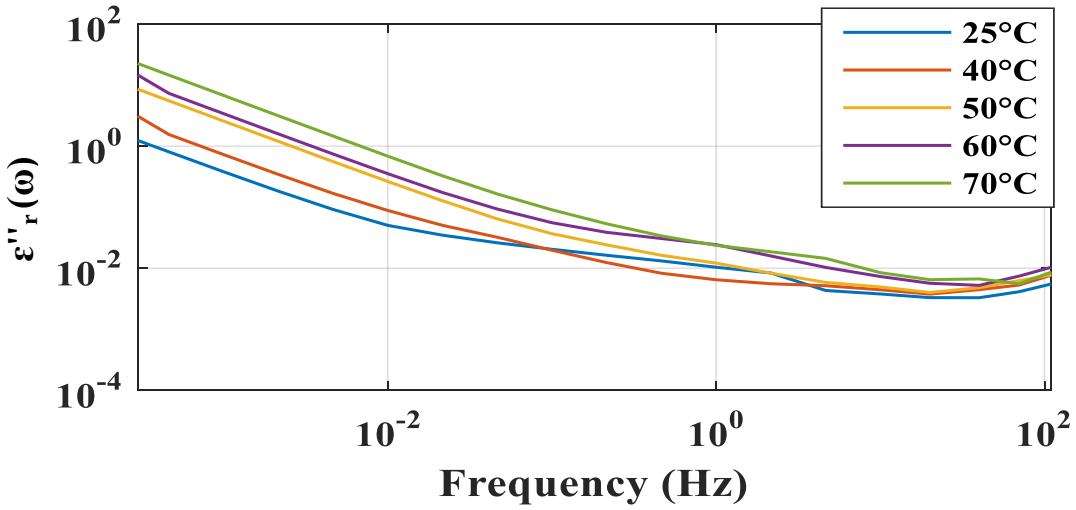

(b)

Fig 5.7. Effect of operating temperature on complex relative permittivity characteristics of XLPE cable (a) real part of complex permittivity (b) imaginary part of complex permittivity

According to Fig 5.7. (a), it is observed that the characteristics of the real part of the complex relative permittivity $\varepsilon'_r(\omega)$ increase with operating temperature increment particularly in the low-frequency region whereas, the characteristics of $\varepsilon'_r(\omega)$ remain unaltered in the high-frequency region. The characteristics of $\varepsilon'_r(\omega)$ with operating temperature variation can be attributed to relative movement of crosslinking polymer chain at high temperature.

According to Fig 5.7. (b), it is observed that the characteristics of the imaginary part of complex relative permittivity $\varepsilon''_r(\omega)$ increase with operating temperature in the entire frequency region. At high operating temperature due to thermal agitation dipoles tend to randomize their orientation. Hence, dipoles cannot react instantly to the applied alternating

field, which leads to more losses at higher operating temperature. It has been discussed in section 3.4 that imaginary part of complex permittivity reflects losses due to conductivity and all kinds of active polarization process in a dielectric material. Therefore, it can be concluded that losses due to d.c. conductivity and active polarization process in XLPE increase remarkably with operating temperature.

Characteristics of the real part of complex permittivity $\varepsilon'_r(\omega)$ and imaginary part of complex permittivity $\varepsilon''_r(\omega)$ for different ppm of water content inside XLPE cable insulation have been shown in Fig 5.8(a) & Fig 5.8(b) accordingly.

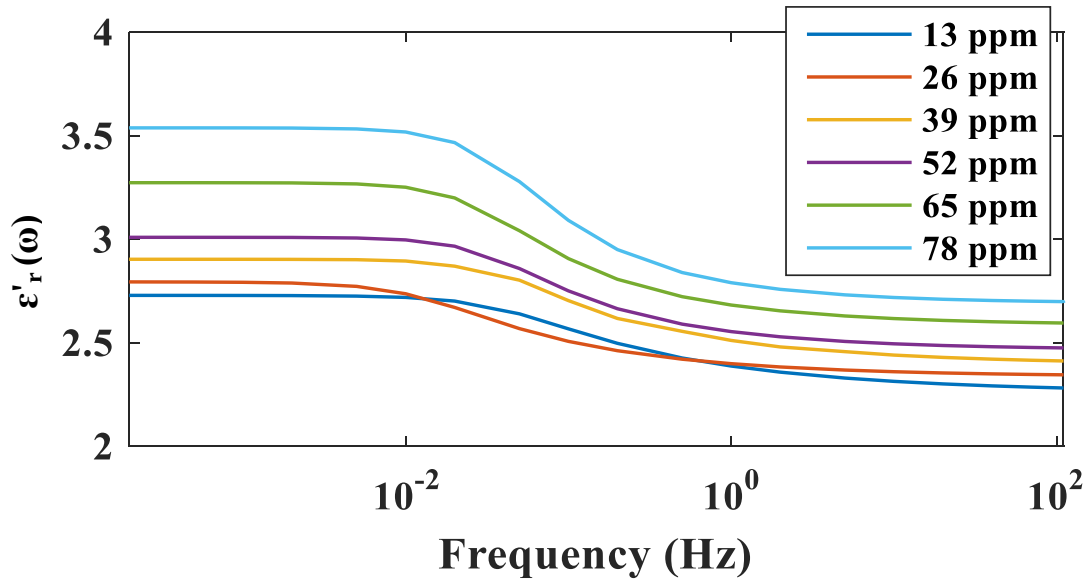

(a)

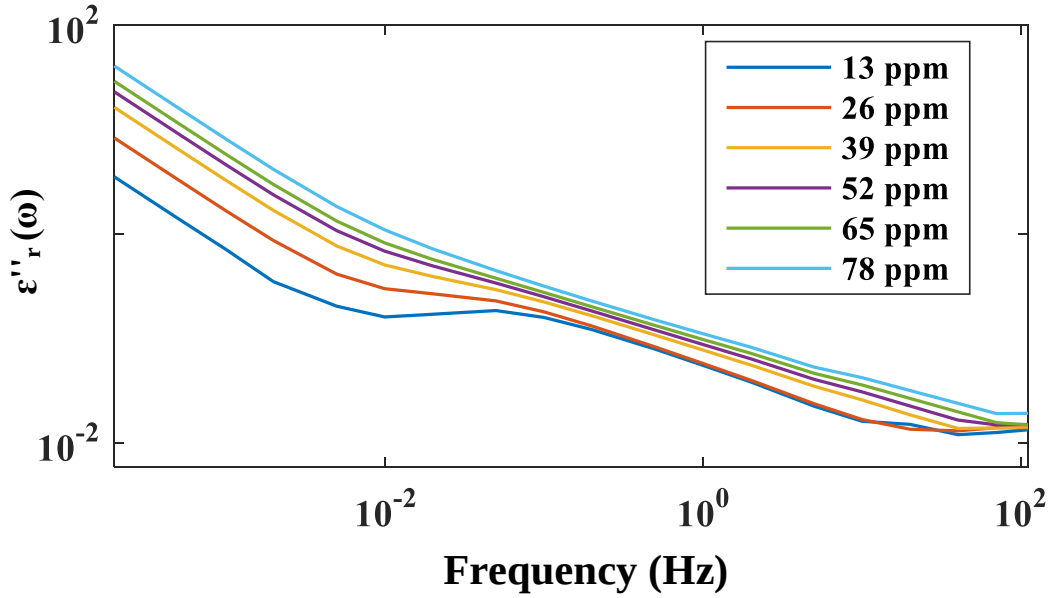

(b)

Fig 5.8. Effect of accumulated water content on complex relative permittivity characteristics of XLPE cable (a) real part of complex permittivity (b) imaginary part of complex permittivity

The effect of water content on the complex permittivity characteristics is depicted by Fig 5.8. According to Fig 5.8 (a), it is observed that $\varepsilon'_r(\omega)$ characteristics tend to increase with the accretion of water content inside cable insulation. This holds true for the entire frequency region. As water exhibits higher dielectric constant (80.4) than XLPE (2.25), thus there is an overall accretion in the real part of relative permittivity characteristics of the cable insulation.

According to Fig 5.8 (b), it is observed that the characteristics of the imaginary part of complex relative permittivity $\varepsilon''_r(\omega)$ increases with the accretion of water content in the entire frequency region. Multiple interfaces are formed inside the insulation due to the injection of water, therefore losses due to interfacial polarization increase remarkably.

CHAPTER-6

MODELING OF XLPE CABLE INSULATION

CHAPTER-6

6.1.INTRODUCTION:

Debye model is one of the popular models to define uniform polarization process in a dielectric. This model proposes an equivalent circuit of insulating material based on the PDC measurement. PDC measurements on XLPE cables are performed by measuring the charging and discharging currents when a step voltage is applied to the XLPE cable insulation and short-circuited after a long time period.

Under the application of an external electric field, dipoles tend to align themselves in the direction of the applied field, which results migration of charge. Therefore, a current will flow inside the insulation due to polarization process. When the field is withdrawn, the dipoles relax and return back to its primary state. In polymeric insulation, each polar group can exhibit a different configuration of neighboring molecules. Hence, the response time of these groups may alter under the application of an electric field [28]. This entire process can be modeled as an electrical circuit, consists of a various number of series R-C branches connected in parallel. The aforementioned equivalent circuit model has been shown in Fig.6.1. Dipoles, which are randomly distributed and involved in active polarization process inside the insulation, are represented by R-C branches in the equivalent circuit model. Apart from current due to active polarization process, polarization current (i_{pol}) also consist conduction current. Conduction current, which can be attributed to insulation resistance of the insulation, is represented by "R_0" in the equivalent circuit model. Current due to delta function is represented by the geometric capacitance of the insulation or "C_0" in this model [28-29].

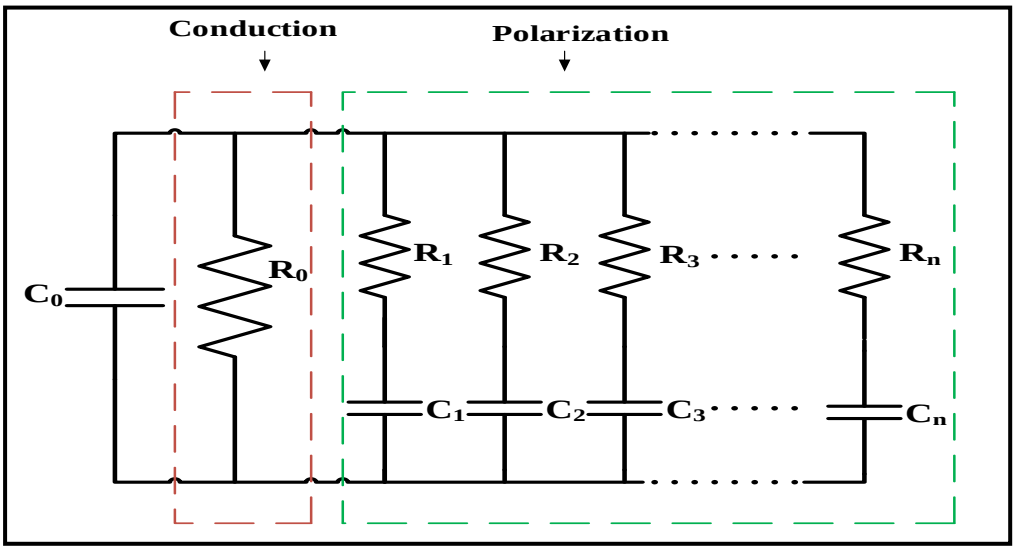

Fig.6.1. Equivalent circuit model of XLPE cable insulation

6.2. CALCULATION OF MODEL PARAMETERS:

Circuit parameters of the Debye model can be derived based on measured polarization and depolarization current. According to the equation (3.16) depolarization current is controlled by dielectric response function, therefore it is more sensible to use depolarization current for the calculation of model parameters rather than polarization current. Depolarization current compromises of different types of active polarization mechanisms inside the insulation. Therefore, the depolarization current can be represented as the summation of the exponentials of the various polarization mechanisms having an individual time constant [28]. Hence, depolarization current $i_{depol}(t)$ can be represented by the equation,

$$i_{depol} = -\sum_{i=1}^{n} A_i e^{-\frac{t}{\tau_i}} \tag{6.1}$$

τ_i is the time constant of each dipole participates in active polarization process, A_i is the decay coefficient of these polarization and n = no R-C branches where,

$$A_i = \frac{U_0}{R_i}(1 - e^{-\frac{t_{pol}}{\tau_i}}) \tag{6.2}$$

$$\tau_i = R_i C_i \tag{6.3}$$

R_0, insulation resistance of the sample, which can be represented as,

$$R_0 \approx \frac{U_0}{i_{pol}(t_{pol}) - i_{depol}(t_{pol})} \tag{6.4}$$

By fitting depolarization current curve with equation (6.1) we can calculate R_i & C_i from equation (6.2) & (6.3). R_0 can be calculated using equation (6.4).

6.3. PROCEDURE AND FLOWCHART OF EQUIVALENT CIRCUIT MODELING:

Depolarization process, which is represented by parallel RC branches on the equivalent circuit, can estimate the dielectric response of the XLPE cable insulation through distributed relaxation times theory. No of parallel RC branches “n” can be derived depending upon the exponential decay shape of the depolarization current curve [29]. To

find no of branches, the depolarization current can be segregated into several segments, as shown in Fig. 6.2.

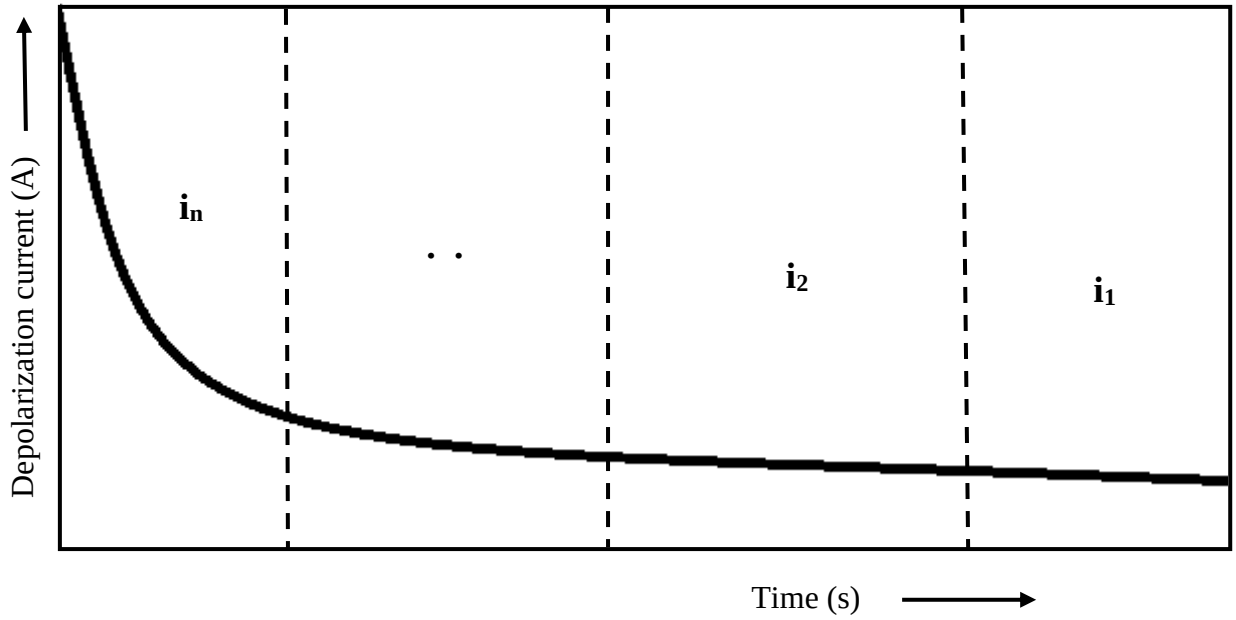

Fig. 6.2. Segregation of depolarization current curve to find no of branches

Branch parameters of the one having the largest time constant can be derived from the final part of the depolarization curve via exponential curve fitting, a form of mathematical regression analysis named least squares method. Once the exponential coefficients due to the branch having a largest time constant are derived, calculated curve based on the derived coefficients is subtracted from the original depolarization curve to get the response for the remaining branches having comparatively smaller time constants. The same procedure is repeated to calculate the branch parameters of the remaining branches having shorter time constants in the descending order. Once the values of A_i and τ_i for all the branches are computed, the values of R_i and C_i can be derived and the equivalent circuit of Debye model can be constructed. The complete procedure of modeling PDC measurement can be summarized in the skeleton of a flowchart, displayed in Fig. 6.3.

In Fig. 6.4 calculated depolarization current curve at 60°C based on the flowchart and the corresponding measured depolarization current have been shown. According to Fig 6.4, the calculated curve almost fits with the measured curve. Similarly, the rest of the measured depolarization current curves are fitted based on the flowchart.

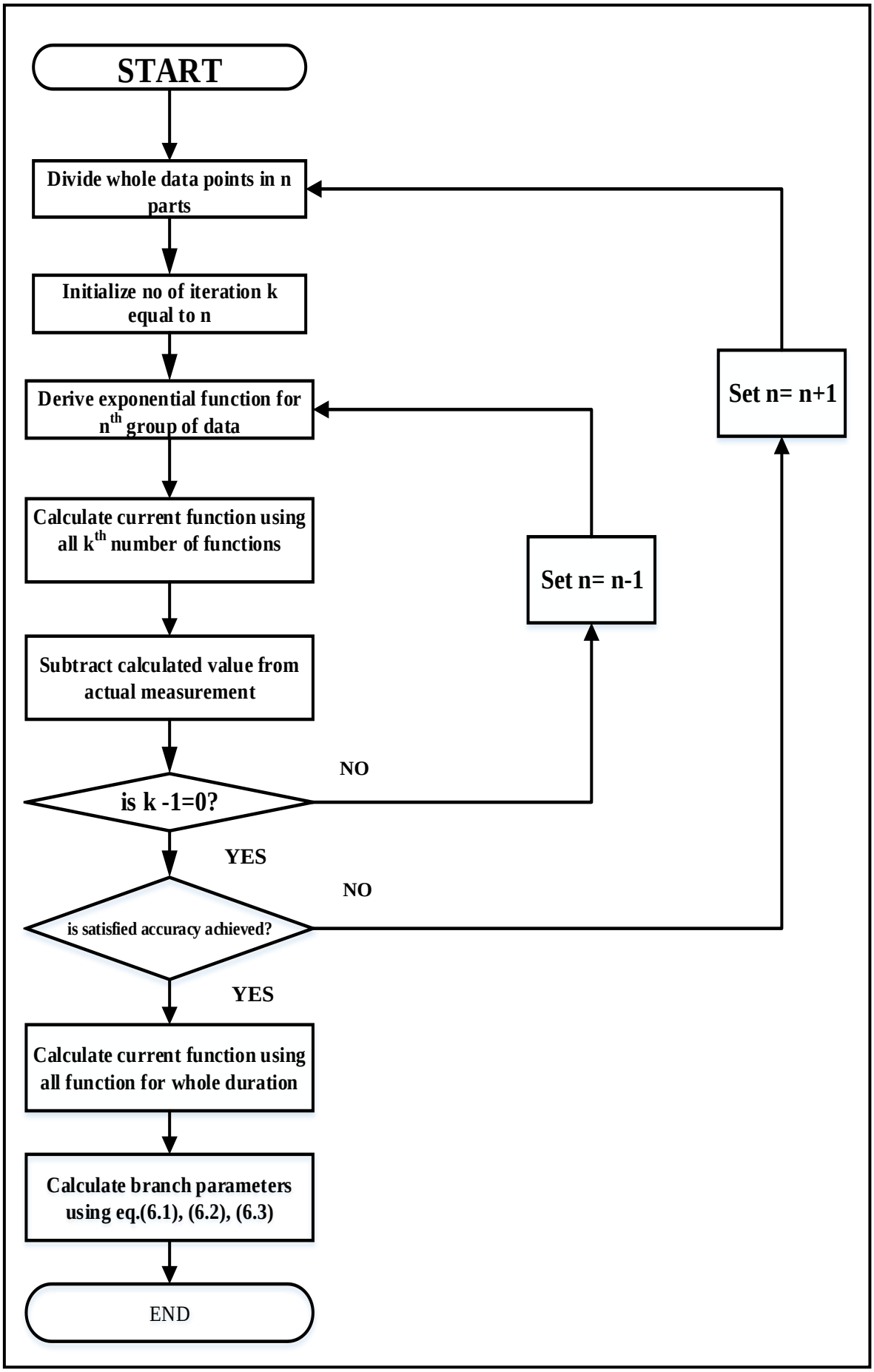

Fig.6.3. Flowchart for the computational procedure

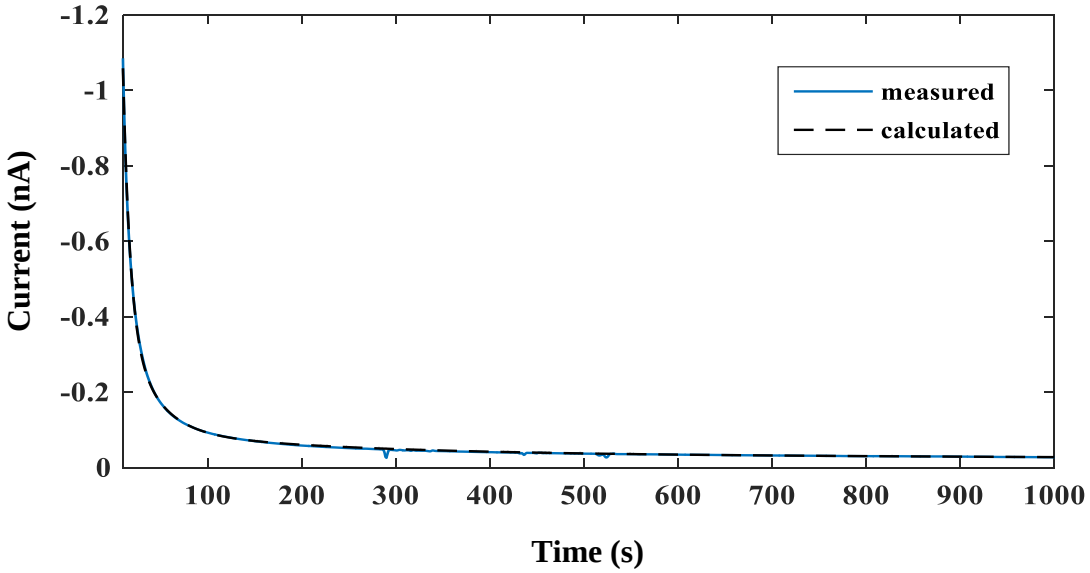

Fig. 6.4. Comparison of calculated and measured depolarization current curve at 60°C

6.4.ESTIMATED RESULT OF DEBYE MODEL BRANCH PARAMETERS:

As discussed in the earlier chapter, PDC measurement has been used to analyse the condition of insulation samples. In the present work PDC data were recorded for the sample at operating temperature (25°C -70°C). Current data were also recorded for the water content variation (13 ppm – 78 ppm) inside the insulation. The data were recorded from t=1sec to t=1000sec under the application of d.c. voltage of 200 V.

Now, on the basis of measured depolarization current curve at each operating temperature the branch parameters of equivalent circuit model, i.e. branch current, time constant, branch resistances and branch capacitors are calculated by using the procedure as discussed in the earlier section. The values of the branch current and respective time constant of each branch for different operating temperatures are represented below in the tabular form. Calculated values of the R-C branch parameters of the equivalent circuit model for different operating temperature are also furnished in Table 6.2.

Table 6.1. Branch current and time constant values for operating temperature variation

Temp (°C)	Branch no (i)	A_i (pA)	τ_i (sec)
25	1	253.5	5.07
	2	46.26	29.33
	3	3.84	899.75
40	1	490.9	8.46
	2	137.9	28.13

	3	52.20	976.21
50	1	2336.4	4.34
	2	518.2	19.67
	3	29.70	686.42
60	1	3360.5	3.92
	2	445.6	37.45
	3	64.63	618.82
70	1	17942.3	2.53
	2	1270.3	16.48
	3	88.2	521.61

Table 6.2. Branch parameters of equivalent circuit model for different operating temperature

Temp (°C)	25	40	50	60	70
R_0 (TΩ)	2.713	1.050	0.806	0.764	0.453
C_0 (pF)	30.22	30.22	30.22	30.22	30.22
R_1 (TΩ)	0.79	0.41	0.085	0.059	0.011
C_1 (pF)	6.64	20.8	51.1	66.6	228.3
R_2 (TΩ)	4.32	1.45	0.385	0.448	0.16
C_2 (pF)	6.79	19.4	53.8	83.6	168.1
R_3 (TΩ)	35.25	24.9	5.16	2.94	1.97
C_3 (pF)	25.8	39.7	133.1	190.9	264.46

In table 6.1 & 6.2 values of branch current (A_i), branch resistance (R_i), branch capacitance (C_i) and branch time constant (τ_i) at different operating temperature has been shown.

Similarly, branch parameters of the equivalent circuit model for different volume of accumulated water content inside cable insulation are calculated through the aforementioned algorithm. Variation of branch parameters of equivalent circuit model, i.e. branch current, time constant, branch resistances and branch capacitors for different water content have been furnished in tabular form in Table 6.3 and Table 6.4 accordingly.

Table 6.3. Branch current and time constant values for different accumulated water content inside insulation

Water Content (ppm)	Branch no (i)	A_i (pA)	τ_i (sec)
13	1	775.1	2.36
	2	41.32	16.47
	3	3.51	1697.75
26	1	2053.4	2.89
	2	84.63	45.7
	3	4.64	1828.28
39	1	1564.6	3.76
	2	169.38	35.87
	3	6.96	2106.6
52	1	2567.44	4.92
	2	320.3	29.35
	3	32.57	1998.4
65	1	2965.3	4.15
	2	345.87	27.03
	3	65.53	2200.6
78	1	3343.3	3.56
	2	563.48	25.69
	3	99.53	2576.5

Table 6.4. Branch parameters for the variation of accumulated water content

Water content (ppm)	13	26	39	52	65	78
R_0 (TΩ)	1.11	0.81	0.59	0.51	0.34	0.28
C_0 (pF)	30.22	30.22	30.22	30.22	30.22	30.22
R_1 (TΩ)	0.258	0.097	0.127	0.078	0.069	0.06
C_1 (pF)	9.15	29.7	29.4	64.8	61.6	59.6
R_2 (TΩ)	4.83	2.63	1.18	0.62	0.58	0.36

C_2 (pF)	**3.41**	**19.4**	**30.4**	**46.9**	**46.8**	**72.3**
R_3 (TΩ)	**25.4**	**18.2**	**10.8**	**2.41**	**1.15**	**0.56**
C_3 (pF)	**66.5**	**99.9**	**195.2**	**826.1**	**1974.3**	**4602.2**

In Table 6.3 & 6.4 values of branch current (A_i) branch resistance (R_i), branch capacitance (C_i) and branch time constant (τ_i) for different accumulated water content inside the insulation have been shown.

6.5.DISCUSSION:

According to the above data table, it is observed that the depolarization current curve is fitted with 3rd other exponential function. So, there exist 3 R-C branches with different time-constant in the equivalent circuit model of XLPE insulation. Therefore, it can be summarized that there exist three types of active polarization process inside insulation. As electronic polarization is very fast polarization process, it can't be modeled through R-C branch. Since XLPE cable is amorphous solid and there exist multiple interfaces between spherules and the amorphous region. Hence, orientation and interfacial polarization process are predominant in XLPE cable. According to Table 6.1, it is observed that branch resistances change considerably with respect to operating temperature. R_1, resistance of the 1st branch is 0.79 TΩ at 25°C which is dipping down to 0.011 TΩ at 70°C, whereas R_2, resistance of the 2nd branch is dipping down from 4.32 TΩ at 25°C to 0.16 TΩ at 70°C and R_3, resistance of the 3rd branch is dipping down from 35.25 TΩ at 25°C to 1.97 TΩ at 70°C. As branch resistances are decreasing with the increment of temperature, hence, the current through each branch is increasing with temperature. Therefore, it can be concluded that with the increment of temperature charge migration inside the insulation due to all kinds of active polarization process is increasing.

According to Table 6.3 and Table 6.4, it is observed that branch parameters change considerably with the variation of accumulated water content. Branch resistances decrease remarkably due to injected water content. It is also observed that branch resistance R_3 decreases more significantly beyond injected water content volume 39 ppm. This can be explained as due to water content multiple interfaces are formed inside the insulation which leads to interfacial polarization. Hence, it can be concluded that current through

branch having larger time-constant i.e. slow polarization process increases predominantly with injected water content.

6.6.ADVANTAGES AND DRAWBACKS:

ADVANTAGES

- Based on this model an insulation system can be represented into an equivalent electrical circuit.
- All types of active polarization process inside the insulation can be segregated and analyzed through this model.
- Dielectric dissipation factor, imaginary capacitance etc. parameters can be computed by converting the equivalent circuit into the frequency domain.

DRAWBACKS

- Through this model, uniform polarization process inside insulation can be analyzed. Since XLPE is amorphous solid, hence polarization process inside the polymeric insulation is non-uniform in nature. Therefore, Debye model is not sufficient to analyze polarization process in polymeric insulation.
- Calculated dissipation factor based on the equivalent circuit parameters doesn't match with measured dissipation factor in the higher frequency region.

CHAPTER-7

DIELECTRIC RELAXATION CHARACTERISTICS OF XLPE CABLE INSULATION

CHAPTER-7

7.1.INTRODUCTION:

Relaxation consists in the recovery of strain on withdrawal of stress. Therefore, it is a time-dependent process, typically under sudden withdrawal or sudden application of stress. The preferable method to analyze the relaxation process is to subject an object to harmonically variable stress or variable frequency stress which is the basics of frequency domain measurement [30].

Relaxation process in solid covers all types of stress relief (dielectric, mechanical, photoconductive, chemical). It is not expected that all these types of relaxation should follow the same laws. Dielectric relaxation process in solid directly depends on the electrical strength of the insulation. Therefore, by analysing dielectric relaxation process in polymeric insulation it is possible to assess the condition of insulation as well as its lifetime under operational conditions [30].

7.2.DIELECTRIC RELAXATION MODELS:

Several models, Debye model [31], Cole-Cole relaxation model [32], Cole-Davidson relaxation model [33], Havriliak-Negami relaxation (H-N) model [34] have been proposed over the years to analyze dielectric relaxation nature in time and frequency domain. Modeling of the dielectric response of insulating material has been done by matching modeled response with experimentally measured values. Practically dielectric relaxation process of a dielectric is a superposition of several individual relaxation processes inside it. In polymeric insulation, it is very difficult to distinguish all individual relaxation process as they often have close relaxation times. Hence, in these models single relaxation time constant has been used.

7.2.1.DEBYE-MODEL OF DIELECTRIC RELAXATION:

Debye model of dielectric relaxation is a classical model, permittivity characteristics of a dielectric can be calculated through the equation given as,

$$\hat{\varepsilon}_r(\omega) = \varepsilon_{r\infty} + \frac{\varepsilon_{rs} - \varepsilon_{r\infty}}{1 + (j\omega\tau_d)} \qquad (7.1)$$

Where, $\hat{\varepsilon}_r(\omega) = \varepsilon'_r(\omega) - j\varepsilon''_r(\omega)$

τ_d is Debye relaxation time constant ε_{rs} is static (low-frequency) dielectric constant whereas, $\varepsilon_{r\infty}$ is high-frequency relative permittivity [35]. If a dielectric follows Debye

relaxation model completely, then the plot between the imaginary part of the complex relative permittivity and the real part of complex relative permittivity, over the entire frequency range forms a semi-circular pattern having its centre point on the X-axis or ε'_r axis. Practically all individual dielectric relaxation processes are not affected the same way with temperature and insulation degradation. Therefore, in many dielectrics, it was observed that the centre point of the semicircle lies beneath the X-axis, which is the limitation of Debye model. Generally, liquid materials maintain a definite molecular structure. Hence, they follow Debye relaxation characteristics [36].

7.2.2.COLE-COLE AND COLE-DAVIDSON MODEL:

In this model deviation to the distributed relaxation nature in dielectrics has been accounted for. This model proposes an analytical modification of Debye relaxation equation. The equation as per the proposed model is given as follows,

$$\hat{\varepsilon}_r(\omega) = \varepsilon_{r\infty} + \frac{\varepsilon_{rs} - \varepsilon_{r\infty}}{1 + (j\omega\tau_{cc})^{1-\alpha}} \tag{7.2}$$

Where the parameter "α" is known as the distribution parameter and "τ_{cc}" is the Cole-Cole relaxation time constant. The parameter α, has a value spanning from 0 to 1 used to characterize the width of relaxation time distribution. For α = 0 Cole –Cole model reduces to Debye model. For α > 0 the relaxation process is dispersed over a wide range of frequency [30]. The value of α can be computed through the ε''_r - ε'_r plot graphically shown in Fig 7.1. If the aforementioned plot exhibits an exact semi-circle with its centre beneath the X-axis, then according to C-C model, the angle made by the centre with the terminal point ($\varepsilon_{r\infty}$) on X-axis can be stated as απ/2.

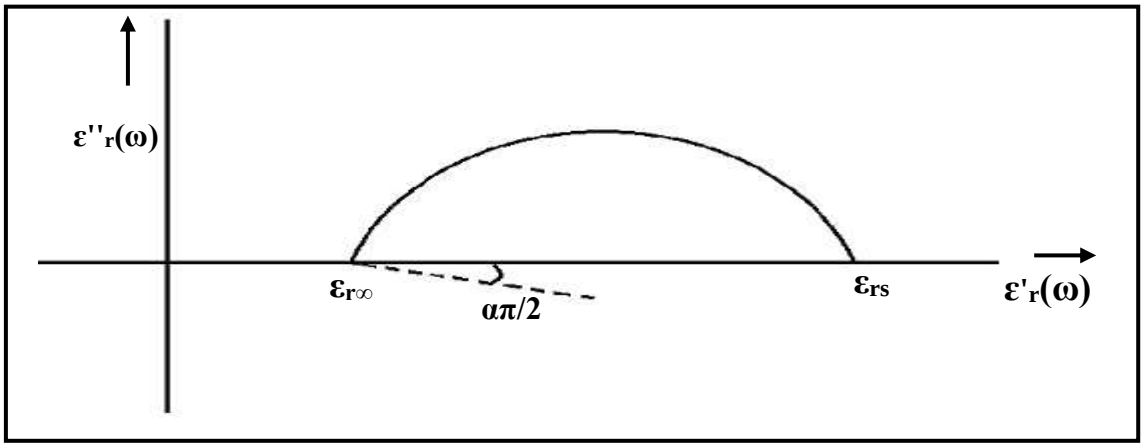

Fig 7.1. Cole –Cole diagram

However, in a polymeric dielectric, it is experimentally observed that the ε''_r - ε'_r plot doesn't follow the semi-circular pattern. In the region near the origin, the plot follows

a straight-line pattern whereas in the region away from the origin it follows the semi-circular pattern. Therefore, another modification in the classical Debye model has been proposed by Cole and Davidson. According to the proposed model permittivity characteristics equation of dielectrics can be given as,

$$\hat{\varepsilon}_r(\omega) = \varepsilon_{r\infty} + \frac{\varepsilon_{rs} - \varepsilon_{r\infty}}{(1 + j\omega\tau_{cd})^{-\beta}} \tag{7.3}$$

Where the parameter "β" is known as "symmetry parameter". It has a value spanning from 0 to 1. The parameter β can be computed from the slope of the straight-line region of the ε''_r - ε'_r plot. If the angle made by the slope of the straight line is φ then, based on the proposed model it can be written as,

$$\varphi = \frac{\beta\pi}{2} \tag{7.4}$$

7.2.3.HAVRILIAK-NEGAMI (H-N) RELAXATION MODEL:

To identify the dielectric relaxation process in amorphous solid like XLPE or composite dielectric an assemble model featuring classical Debye model, Cole-Cole model and Cole-Davidson model has been proposed by Havriliak and Negami. Permittivity characteristics equation of dielectrics according to the proposed model can be given as,

$$\hat{\varepsilon}_r(\omega) = \varepsilon_{r\infty} + \frac{\varepsilon_{rs} - \varepsilon_{r\infty}}{(1 + (j\omega\tau_{hn})^{1-\alpha})^{-\beta}} \tag{7.5}$$

Where "τ_{hn}" is the Haviriliak-Negami relaxation time constant. According to equation (7.5), it is observed that Cole-Cole model and Cole-Davidson model is the special cases of H-N model. For α=0, β=0 aforementioned equation represents Debye relaxation model, for α>0, β=0 aforementioned equation represents Cole-Cole relaxation model, for α=0, β<1 aforementioned equation represents Cole–Davidson relaxation model. Due to the inherent flexibility of H-N model, it is suitable for analysing dielectric relaxation nature of polymeric insulation at different temperature as well as the effect of water content inside the insulation based on frequency domain spectroscopy [29, 32].

7.3. GRAPHICAL METHOD OF HAVRILIAK–NEGAMI PARAMETER CALCULATION:

It has been found that for analysing the dielectric properties of polymeric insulation like XLPE, electrical susceptibility (χ) is more suitable than relative permittivity (ε_r), which is more applicable for analysing dielectric characteristics in a capacitor.

Since, $\chi'(\omega)$ and $\chi''(\omega)$ are the real and imaginary parts of complex susceptibility, then the ε''_r - ε'_r plot can be transformed into the plot of $\chi''(\omega)$ versus $\chi'(\omega)$ using the equation (3.22) and (3.23) if the value of d.c. conductivity (σ_0) is known. Once the d.c. conductivity (σ_0) part has been subtracted, what is left in the plot is purely due to dielectric polarization processes.

The present work is aimed to identify the effect of operating temperature and water content inside XLPE insulation, therefore H-N model has been applied on the $\chi''(\omega)$ versus $\chi'(\omega)$ plot at different temperature and different stages of accumulated water content inside the insulation. For this purpose, equation (7.5) has been slightly modified to the following equation given as,

$$\hat{\chi}(\omega) = \chi_\infty + \frac{\chi_s - \chi_\infty}{(1 + (j\omega\tau_{hn})^{1-\alpha})^{-\beta}} \tag{7.6}$$

Where χ_s and χ_∞ are static and high-frequency electrical susceptibility of the insulation system respectively.

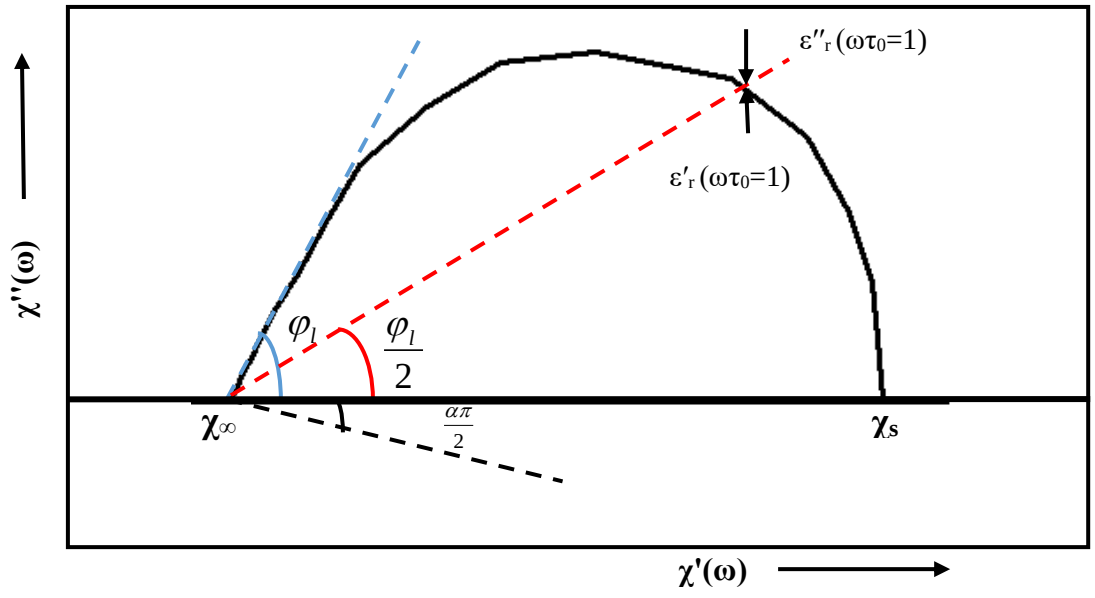

Fig.7.2. Graphical representation of $\chi''(\omega)$ vs $\chi'(\omega)$ plot of H-N model

As discussed in the earlier section distribution parameter "α" can be computed graphically from the ε''_r - ε'_r plot. However, determination of symmetry parameter "β" through the equation (7.4) is no longer applicable in case of H-N model [34]. If the angle made by the slope of straight-line section in the $\chi''(\omega)$ -$\chi'(\omega)$ plot is φ_l, then

$$\beta = \frac{2\varphi_l}{\pi(1-\alpha)} \tag{7.7}$$

The complete algorithm of the graphical method for calculating H-N model parameters is given as follows,

Step-1

At lower frequency (0.2 mHz), applied sinusoidal voltage can be compared as d.c. source. Hence, equation (3.23) can be expressed as,

$$\varepsilon''_r(\omega) \approx \frac{\sigma_0}{\varepsilon_0 \omega}$$

Therefore, based on the aforementioned equation, d.c. conductivity (σ_0) can be estimated.

Step-2

$\chi'(\omega)$ and $\chi''(\omega)$ are derived using equation (3.22) & (3.23) and plotted along X & Y axis accordingly.

Step-3

Co-ordinates of χ_s and χ_∞ are initialized from the $\chi''(\omega)$ vs $\chi'(\omega)$ plot.

Step-4

Low-frequency data of $\chi''(\omega)$-$\chi'(\omega)$ plot is fitted with semi-circle to find the centre point. According to Fig.7.2 α can be computed from the angle made by the centre of the semi-circle with χ_∞ on X-axis.

Step-5

From the slope of high-frequency data of $\chi''(\omega)$-$\chi'(\omega)$ plot φ_l is calculated and based on the equation (7.7) magnitude of β is determined.

Step-6

The parameter τ_{hn} also can be computed graphically. Bisector of angle φ_l will intersect $\chi''(\omega)$-$\chi'(\omega)$ plot at a certain point. Co-ordinate of the point will indicate particular values of $\varepsilon'_r(\omega)$ and $\varepsilon''_r(\omega)$. If the corresponding frequency of the intersection point is ω_{hn} then the parameter τ_{hn} is calculated using the following relation.

$$\omega_{hn}\tau_{hn} = 1$$

Step-7

Once α, β and τ_{hn} have been calculated, the real and imaginary part of complex susceptibility can be determined using the equation (7.6). The values of $\chi''_{cal}(\omega)$ and $\chi'_{cal}(\omega)$ are compared with measured values of $\chi''(\omega)$ & $\chi'(\omega)$.

Step-8

If calculated values don't fit with measured values then τ_{hn} is optimized and repeat step-4 to calculate α with more no of low-frequency data until satisfied accuracy is achieved. The optimization technique used is non-linear least square optimization (NLSO) [33].

7.4. FITTING OF MODEL PARAMETERS AND RESULT:

This chapter is aimed at identifying the effect of the operating temperature and water content on the dielectric relaxation characteristics of XLPE cable insulation. Hence, data obtained through the FDS measurement is fitted with the characteristics equation of H-N model. The methodology of identifying the model parameters has been discussed in the earlier section.

7.4.1. OPERATING TEMPERATURE VARIATION:

Calculated $\chi''(\omega)$-$\chi'(\omega)$ characteristics through FDS measurement and corresponding fitted $\chi''(\omega)$-$\chi'(\omega)$ characteristics of XLPE cable at different operating temperature have been displayed in Fig 7.3.

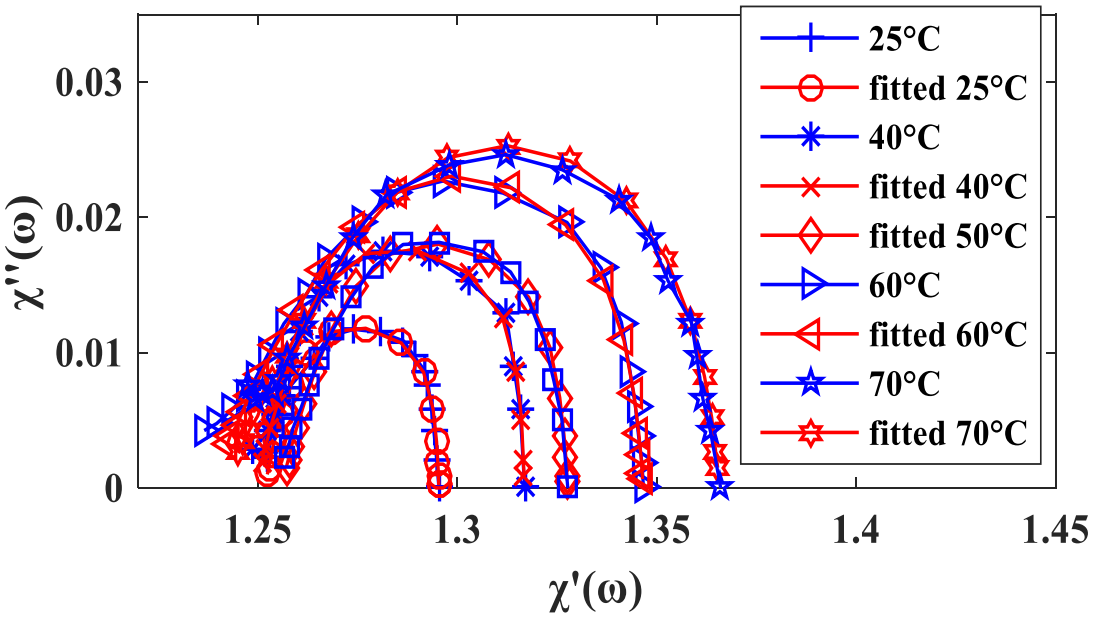

Fig.7.3. Measured and fitted χ''(ω) vs χ'(ω) characteristics at different operating temperature

According to Fig.7.3, it is observed that $\chi''(\omega)$ vs $\chi'(\omega)$ plot shifts towards the right with the increment of operating temperature. It is also observed that the gap between static susceptibility (χ_s) and high-frequency susceptibility (χ_∞) in the $\chi''(\omega)$ vs $\chi'(\omega)$ plot and the peak of $\chi''(\omega)$ vs $\chi'(\omega)$ plot increases with the temperature increment. The calculated result of H-N model parameters i.e. α, β, τ_{hn} has been furnished in the tabular form shown in Table 7.1.

Table 7.1. Variation of model parameters with operating temperature

Temperature (°C)	**α**	**β**	**τ_{hn}**
25	**0.076**	**0.574**	**9.16**
40	**0.094**	**0.523**	**9.23**
50	**0.103**	**0.502**	**9.13**
60	**0.207**	**0.463**	**9.05**
70	**0.282**	**0.411**	**9.12**

From Table 7.1, it is observed that the value of "α" is increasing and "β" is decreasing with temperature. Relaxation time constant "τ_{hn}" is almost unchanged with temperature. As the value of α and increasing and β is decreasing with operating temperature so, it can be stated that with temperature increment dielectric relaxation characteristics in XLPE deviates from Debye characteristics. This can be explained as, with temperature long polymeric chain of XLPE will break and due to thermal oxidation, a lot of hydroxyl group is generated, also dipoles randomize their orientation at higher operating temperature due to thermal agitation. Multiple micro interfaces between spherulites and the amorphous region inside XLPE insulation are also formed during over-heating. Due to the shorter length and lower mass newly formed polymeric chains after chain scissions are more flexible to orient according to the applied electric field.

The variation of α and β with operating temperature has been plotted in Fig.7.4 (a) and Fig.7.4 (b) accordingly.

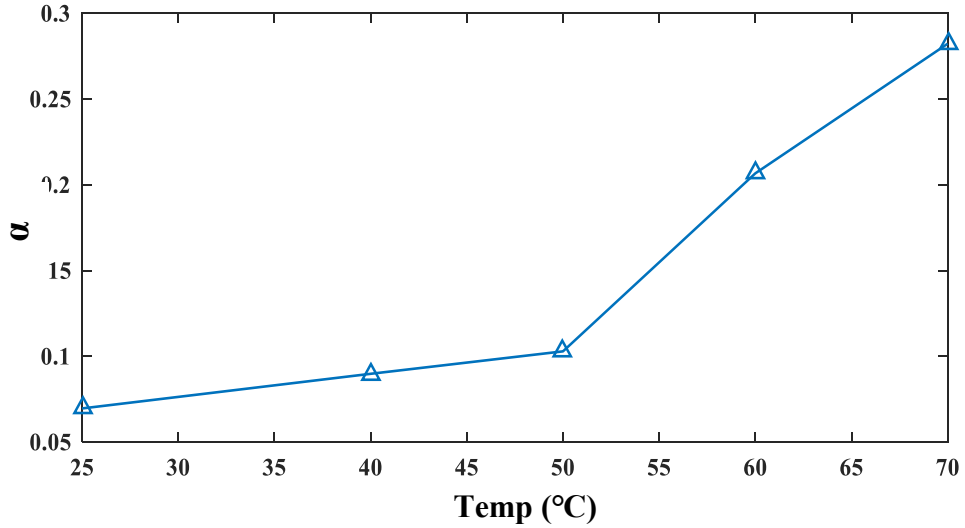

(a)

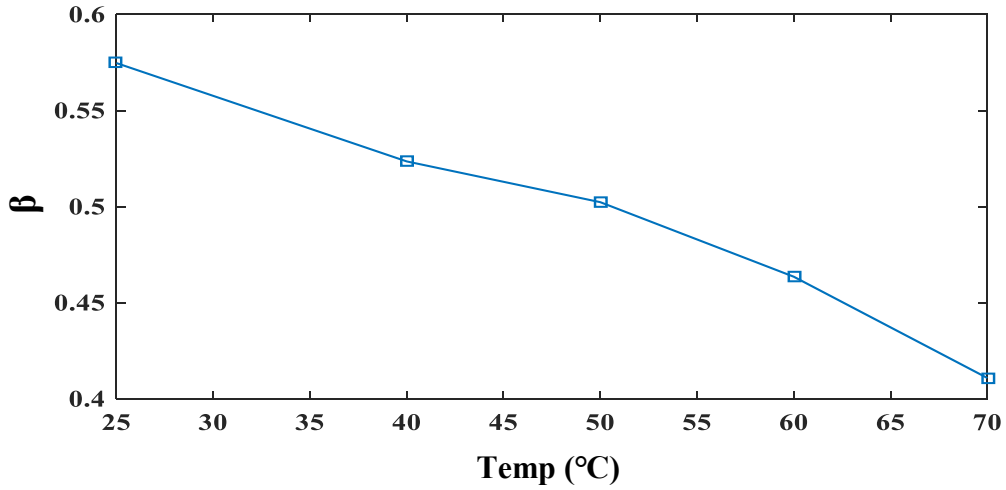

(b)

Fig. 7.4. Variation of model parameters with operating temperature (a) variation of α with operating temperature (b) variation of β with operating temperature

Based on the regression method, the relationship between α and operating temperature can be obtained, which has been shown in the following equation.

$$\alpha = a_1 + a_2 t + a_3 t^2 \tag{7.8}$$

Where "t" is referred as operating temperature in °C. The value of coefficients obtained using the regression method has been shown in Table 8.2. The calculated R-square value is 0.978.

Similarly using the regression method, a relationship between β and operating temperature can also be derived which has been written in the equation (7.9)

$$\beta = b_1 + b_2 t + b_3 t^2 \tag{7.9}$$

Value of the coefficients "a_1, a_2, a_3, b_1, b_2 and b_3" have been shown in Table 7.2.

Table 7.2 Coefficients of fitting parameters

a_1	a_2	a_3	b_1	b_2	b_3
0.1908	**-8.244×10^{-3}**	**1.374×10^{-4}**	**0.6114**	**-0.0008817**	**-2.768×10^{-5}**

Based on the equation (7.8) and (7.9), the magnitude of α & β can be computed at any temperature between 25°C-70°C without performing the experiment.

Comparison between measured dissipation factor curve and calculated dissipation factor curve based on H-N model for different operating temperature are shown in Fig. 7.5.

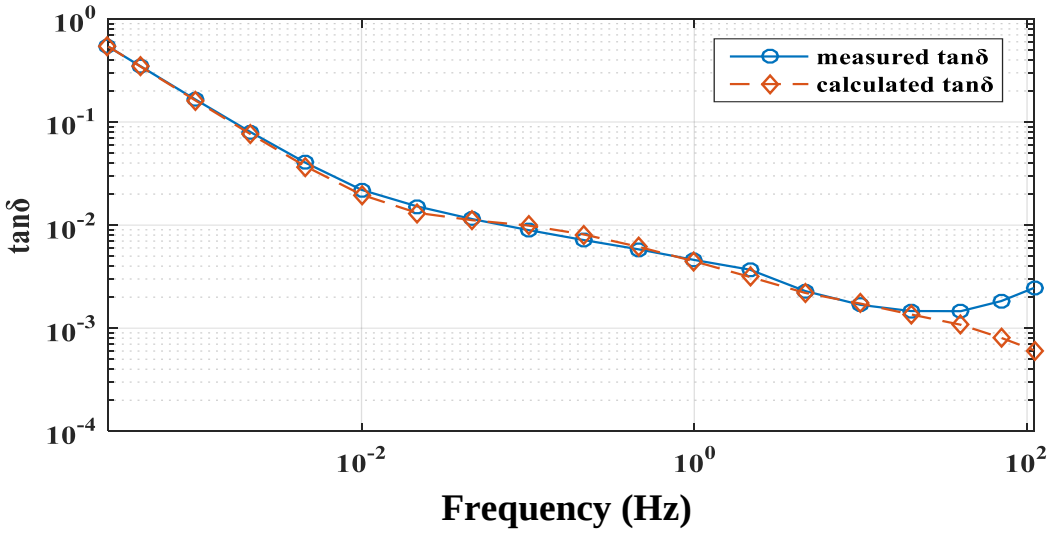

(a)

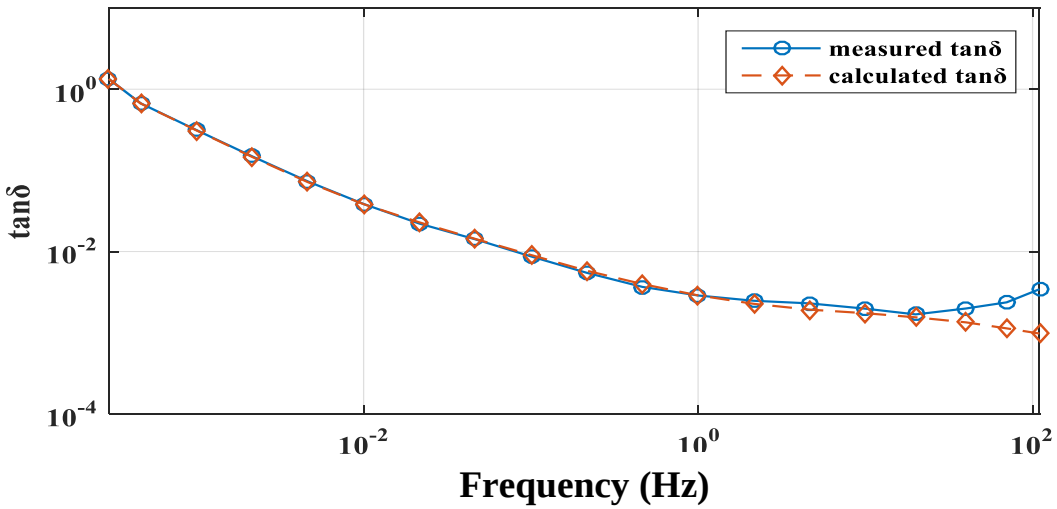

(b)

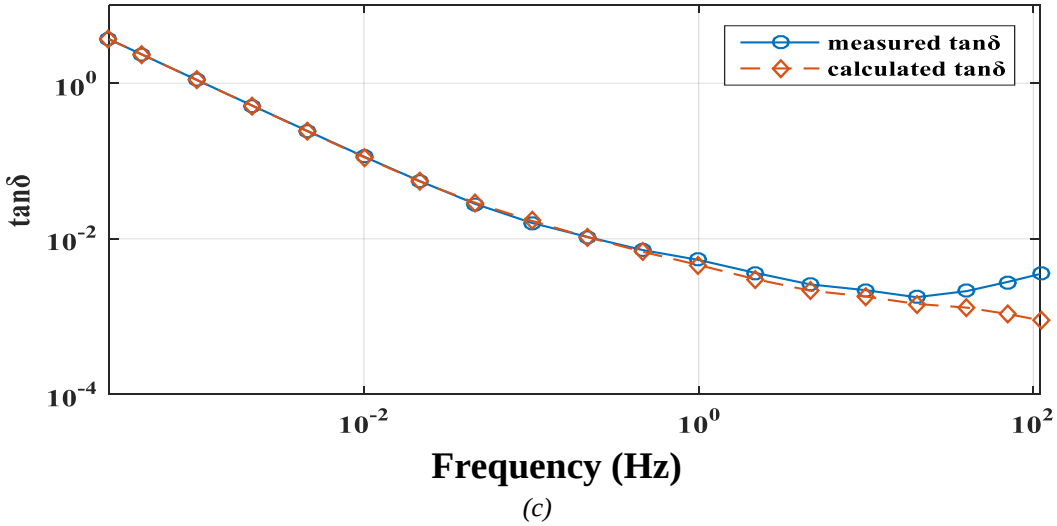

(c)

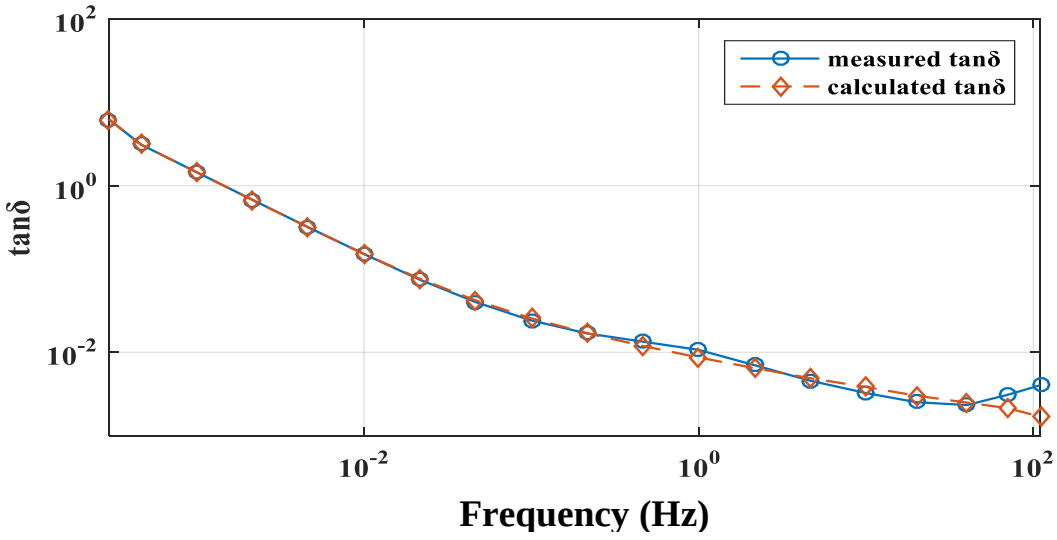

(d)

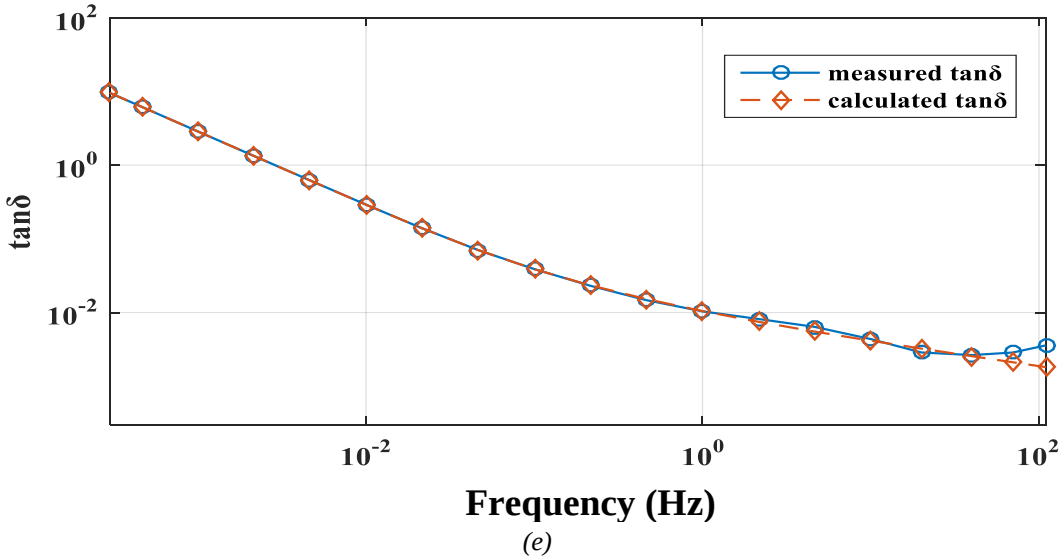

(e)

Fig.7.5.Measured and calculated tanδ curves based on H-N model at (a) 25°C, (b) 40°C, (c) 50°C, (d) 60°C and (e) 70°C

According to Fig.7.3 & Fig.7.5, it is observed that measured characteristics for different operating temperature and modeled characteristics based on H-N model almost matched. Though model characteristics deviate from measured characteristics in the higher frequency region. As discussed in the section 5.4, tanδ or dissipation factor starts to increase in the higher frequency region. Hence, higher frequency data have been excluded from this model. Percentage error between measured dissipation factor and calculated dissipation factor based on H-N model can be shown as,

$$\%error = \frac{\tan\delta_{cal}(\omega) - \tan\delta_{m}(\omega)}{\tan\delta_{m}(\omega)} \times 100$$

Mean absolute error between the measured dissipation factor and the calculated dissipation factor curves at each operating temperature has been shown in Table 7.3.

Table 7.3 Percentage mean absolute error between measured and calculated tanδ curves for different operating temperature

Temp (°C)	Mean absolute error (%)
25	**8.09**
40	**8.25**
50	**9.67**
60	**5.85**
70	**4.46**

7.4.2. WATER CONTENT VARIATION:

Calculated $\chi''(\omega)$-$\chi'(\omega)$ characteristics through FDS measurement and the corresponding fitted characteristics of varying water content inside the insulation are shown in Fig 7.6.

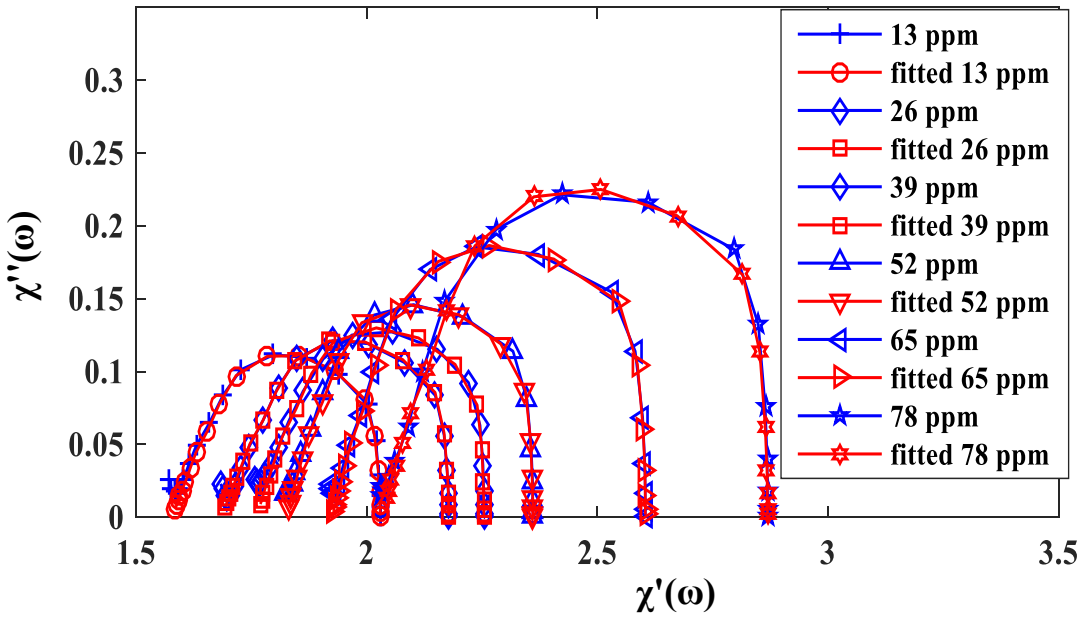

Fig. 7.6. χ''(ω) vs χ'(ω) plot for water content variation

According to Fig.7.6, it is observed that χ''(ω) vs χ'(ω) plot shifts towards the right with the injection of contaminated water inside cable insulation. It is also observed that the gap between static susceptibility (χ_s) and high-frequency susceptibility (χ_∞) in the χ''(ω) vs χ'(ω) plot and the peak of χ''(ω) vs χ'(ω) plot also increases with the accretion of water content inside the insulation. Therefore, overall polarization process increases due to accumulated water inside the insulation. The calculated result of H-N model parameters i.e. α, β, τ_{hn} has been shown in tabular form in Table 7.4.

Table 7.4 Model parameters for the variation of accumulated water content inside XLPE insulation

Water content (ppm)	α	β	τ_{hn}
13	0.0736	0.452	10.8
26	0.0582	0.486	9.67
39	0.0409	0.506	8.51
52	0.0326	0.529	7.69
65	0.0202	0.548	6.67
78	0.0104	0.559	6.04

According to Table 7.4, it is observed that with the injection of contaminated water inside the insulation value of α in decreasing and β is increasing. Since liquid materials follow Debye characteristics, so based on the results of α and β, it can be concluded that with the accretion of water content dielectric relaxation characteristics of the XLPE

insulation gravitates towards Debye characteristics. The relaxation time constant (τ_{hn}) is also decreasing with the accretion of water content as water forms a conducting path inside the insulation.

Specific values of water content inside the cable insulation are plotted against the corresponding calculated values of α and β in a three-dimensional curve. Aforementioned 3D curve is shown in Fig. 7.7.

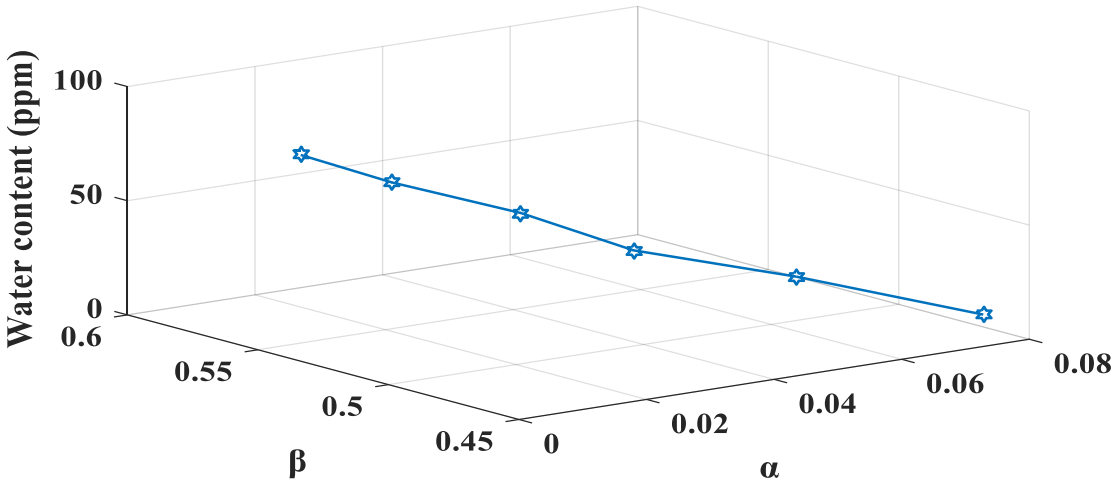

Fig 7.7. 3D plot for water content with respect to the variation of α and β

Variation of relaxation time constant (τ_{hn}) with water content has been displayed in Fig. 7.8.

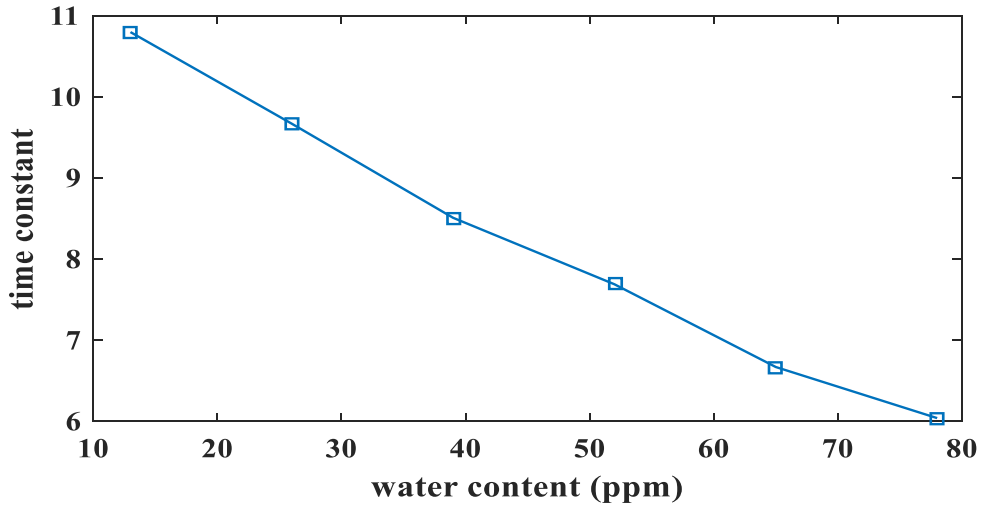

Fig. 7.8. Variation of τ_{hn} with injected water content

Measured tanδ curve and corresponding calculated tanδ curve based on H-N model for different water content have been shown in Fig 7.9.

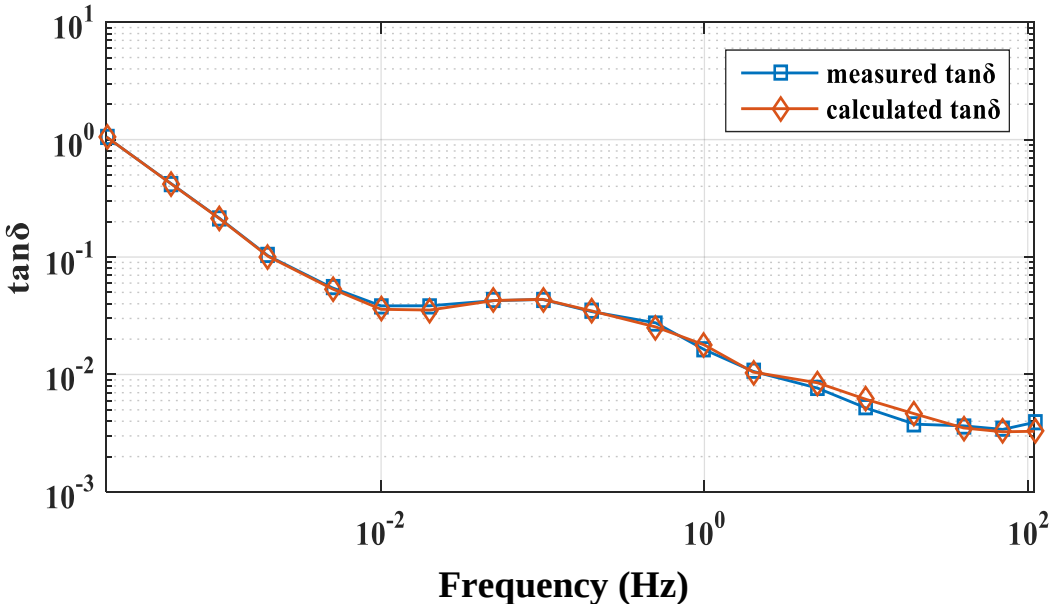
measured tanδ
calculated tanδ
tanδ
Frequency (Hz)

(a)

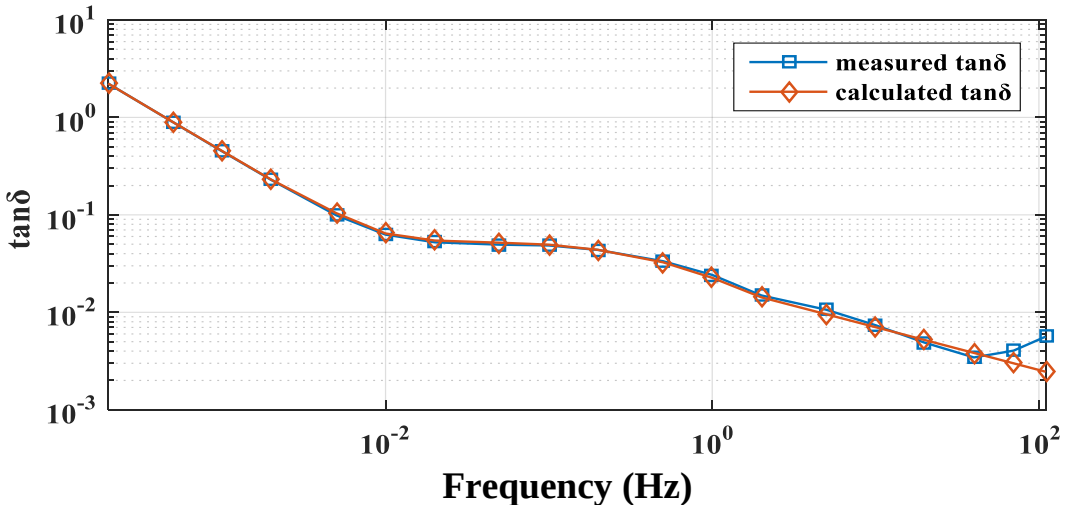
measured tanδ
calculated tanδ
tanδ
Frequency (Hz)

(b)

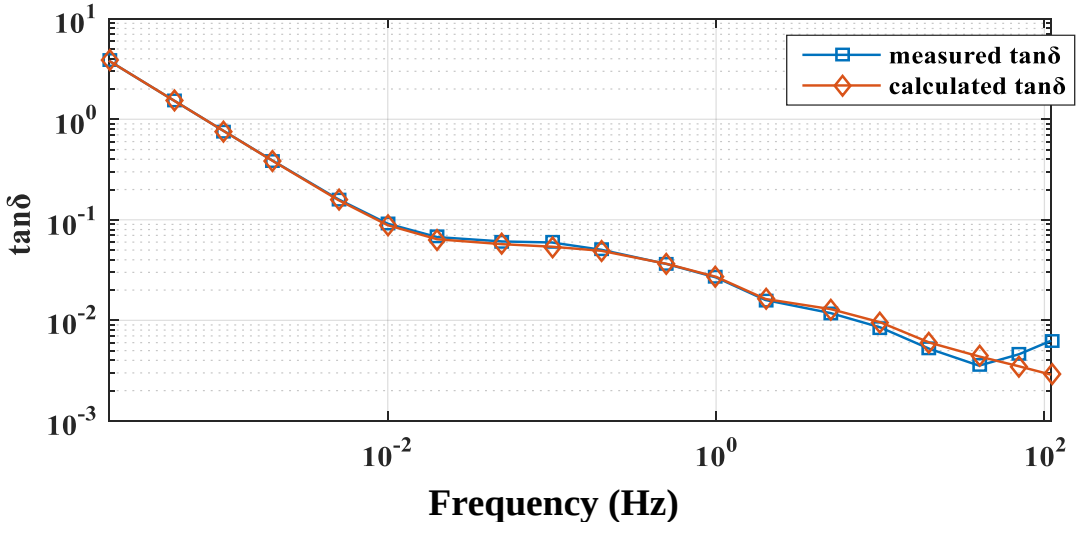
measured tanδ
calculated tanδ
tanδ
Frequency (Hz)

(c)

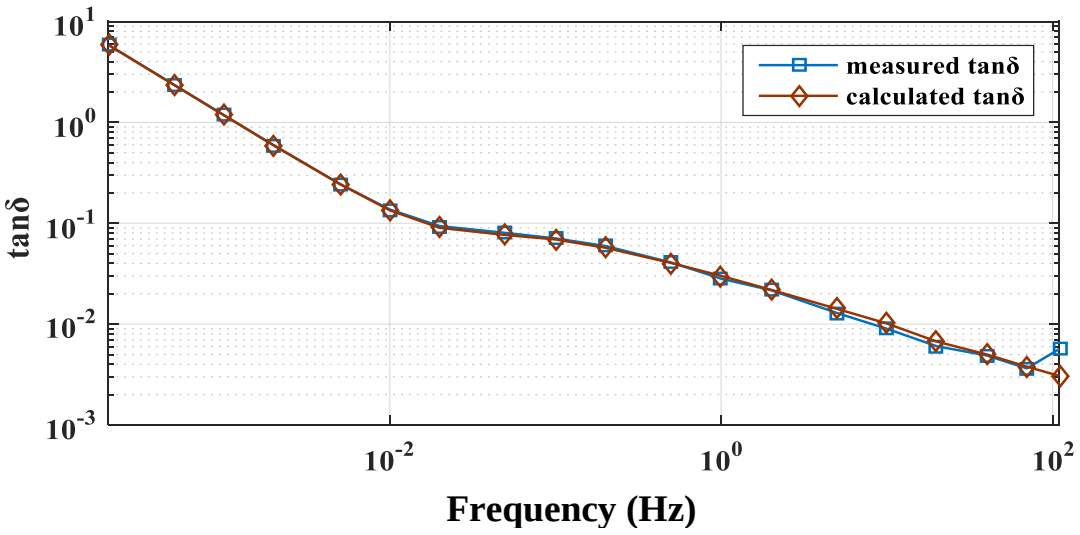

(d)

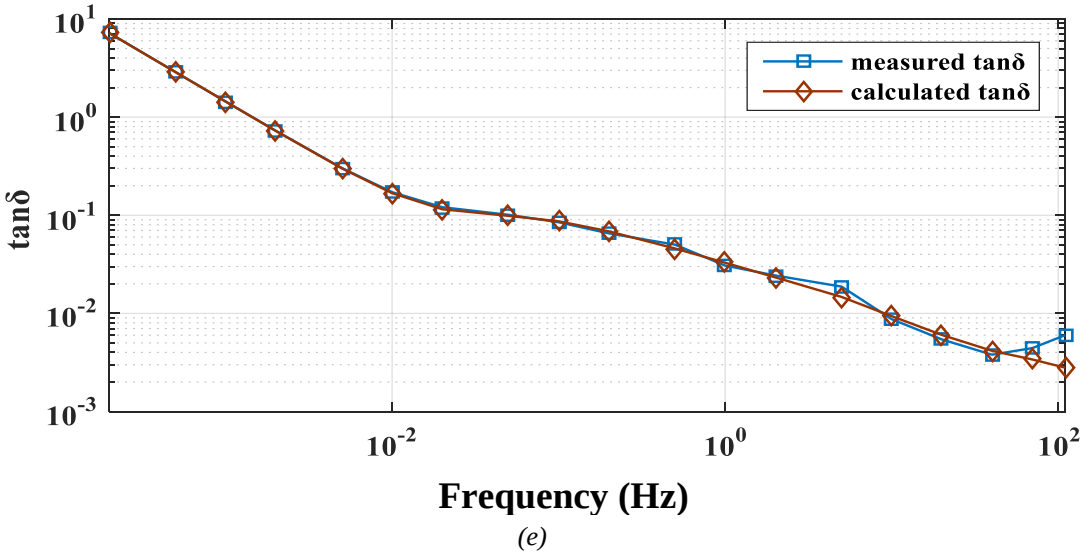

(e)

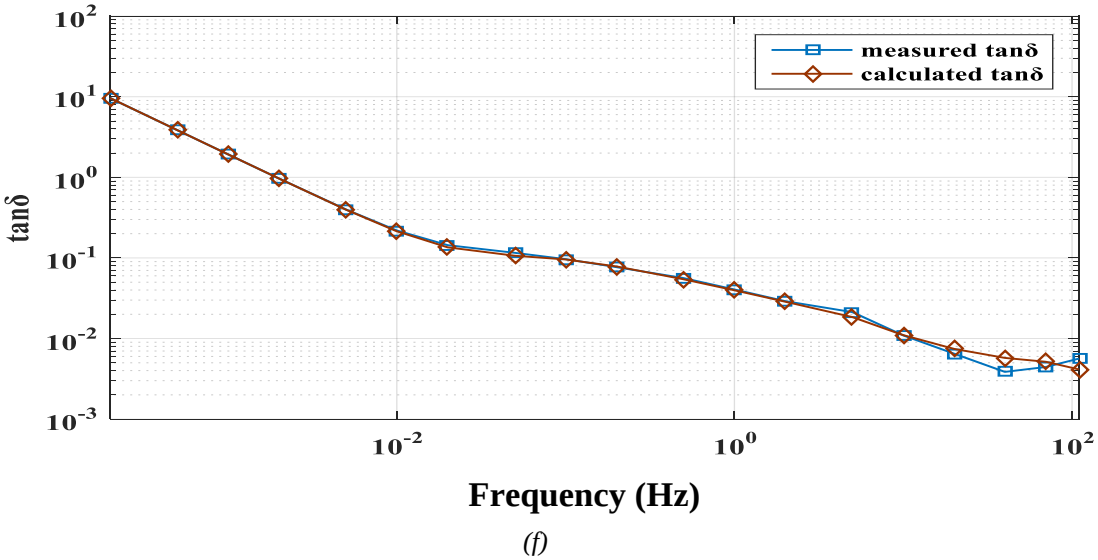

(f)

Fig 7.9. Measured and calculated tanδ curves based on H-N model at water content (a) 13 ppm, (b) 26 ppm, (c) 39 ppm, (d) 52 ppm, (e) 65 ppm and (f) 78 ppm

According to Fig 7.6 & Fig 7.9, it is observed that the measured characteristics for different content of water inside cable insulation and the modeled characteristics based on H-N model almost matched. Though model characteristics deviate from the measured characteristics in the higher frequency region.

The mean absolute error between measured dissipation factor and calculated dissipation factor curves based on H-N model for water content variation have been shown in Table 7.5.

Table 7.5. Percentage mean absolute error between measured and calculated tanδ curves for different water content inside cable insulation

Water content (ppm)	Mean absolute error (%)
13	**7.35**
26	**5.30**
39	**6.13**
52	**5.33**
65	**6.56**
78	**5.46**

7.5.*CONCLUSION:*

Therefore, it can be concluded that dielectric relaxation characteristics of XLPE cable insulation can be assessed at different operating temperature and water content on the basis of calculated parameters "α, β and τ_{hn}". The methodology described in this model to identify dielectric relaxation characteristics is quite straightforward, conclusive and can be employed using non-invasive means.

CHAPTER-8

ESTIMATION OF WATER CONTENT IN XLPE CABLE

CHAPTER-8

8.1.INTRODUCTION:

In the earlier chapter, it has been discussed that water tree is one of the primary causes of insulation failure in XLPE cable. As water tree degradation is a slow process, therefore over the years water content inside cable insulation increases which leads to the escalation of dielectric loss. This chapter is aimed at estimating the water content inside the insulation, which is suitable to investigate insulation condition of cable at different stages of water tree. Dissipation factor measured at power frequency ($\tan\delta_{pwr}$) is an aging sensitive parameter, which is usually employed as an indicator of insulation status [39]. Dissipation factor measured at power frequency, $\tan\delta_{pwr}$ being less sensitive to insulation geometry provides several advantages. The value of moisture content inside insulation can be expressed in terms of minimum dissipation factor $\tan\delta_{min}$ obtained by applying variable frequency alternating field [40]. Similarly, water content inside the insulation can also be expressed in terms of minimum dissipation factor. Dissipation factor measured at power frequency represents the total dielectric loss, hence is influenced by both water content as well as by thermal/aging conductive by-products. According to equation 3.24, dissipation factor directly depends on the losses due to the d.c. conductivity and the polarization process. At power frequency, losses due to the d.c. conductivity is very small compared to losses due to the polarization process, hence, it seems more logical that $\tan\delta_{pwr}$ will be influenced by losses due to the polarization process. As accumulated water inside XLPE cable creates multiple interfaces with water tree aging, thus it can be stated that losses due to the polarization process also increases, which reflects an escalation of dissipation factor in the power frequency range.

8.2.ESTIMATED RESULT OF WATER CONTENT:

Measured dissipation factor curve at different water content inside the cable insulation employing the frequency domain spectroscopy has been shown in Fig 5.6. (Chapter 5). According to Fig 5.6, it is observed that the minima of the dissipation factor curve lies in the power frequency region, thus it seems more sensible to correlate $\tan\delta_{min}$ with the water content inside the XLPE cable. Minimum dissipation factor and its corresponding frequency based on the FDS data for different value of the water content (θ_w) have been shown in tabular form in Table 8.1.

Table 8.1. Minimum tanδ and its corresponding frequency for different water content

Water content (θ_w) (ppm)	$\tan\delta_{min}$	Corresponding frequency (Hz)
13	**0.003389**	**70**
26	**0.003445**	**40**
39	**0.003543**	**40**
52	**0.003646**	**70**
65	**0.003792**	**40**
78	**0.003875**	**40**

Based on the least square method, water content inside XLPE cable can be correlated with $\tan\delta_{min}$ using the following equation,

$$\theta_{w\,estimated}\ (ppm) = k_1 + k_2 \ln(\tan\delta_{\min}) \tag{8.1}$$

Where, $k_1 = 2.61\times10^3$ and $k_2 = 455.9$

Calculated R-square value=0.988

The value of volumetric water content inside cable insulation at different stages of its service life can be estimated using equation 8.1. The percentage error on estimating the water content inside cable insulation has also been evaluated using equation 8.2 and shown in Table 8.2.

$$\%error = \frac{\left|\theta_{westimated} - \theta_{wactual}\right|}{\theta_{wactual}} \times 100 \tag{8.2}$$

Table 8.2. Estimated water content using (8.1) and corresponding estimated error

Actual Water content ($\theta_{w\,actual}$) (ppm)	$\tan\delta_{min}$	Estimated water content ($\theta_{w\,estimated}$) (ppm)	Error (%)
13	**0.003389**	**17.19**	**32.23**
26	**0.003445**	**24.67**	**5.11**
39	**0.003543**	**37.49**	**3.87**
52	**0.003646**	**50.52**	**2.84**
65	**0.003792**	**68.42**	**5.26**
78	**0.003875**	**78.29**	**0.37**

8.3.CONCLUSION:

Results reported in this chapter suggested that the proposed methodology can improve the reliability of assessing the condition of water tree aged cable besides being cost-effective. If the measured dissipation factor of a cable under service is anything less than 0.00325 then based on equation 8.1, it can be concluded that the cable is unaffected by water tree aging i.e. water content inside the insulation is zero. According to Table 8.2, it is observed that the error in the predicted water content is significantly high for the cable containing relatively less amount of water. Hence, accurate prediction of water content inside cable insulation of the relatively new cable based on this method is not reliable. It is practically difficult to ascertain beforehand whether the accumulated water content inside cable insulation is high or low. Hence, the prediction of water content inside cable insulation based on $\tan\delta_{min}$ based relationship always includes a degree of uncertainty, especially for the relatively new cable.

CHAPTER-9

CONCLUSION AND FUTURE SCOPE

CHAPTER-9

9.1.CONCLUSION:

The experimental conditions for the investigation of dielectric response of Single-core XLPE cable insulation were done in the High Tension Laboratory, Jadavpur University, at a different operating temperature ranging from 25°C to 70°C and water content inside the insulation ranging from 13 ppm to 78 ppm. The responses were recorded in time domain through polarization and depolarization current and in frequency domain through frequency domain spectroscopy.

In this work, an equivalent circuit model of XLPE cable insulation has been modeled through PDC measurement to investigate different kinds of active polarization process inside the insulation. Based on this model, it is found that the dielectric response of the XLPE cable can be represented through three sets of R-C branches in the equivalent circuit model. Hence, it can be concluded that there exists three different kinds of active polarization process inside the XLPE insulation. It is also observed that branch parameters of the equivalent circuit model change remarkably with operating temperature and accumulated water content inside the insulation.

To investigate the dielectric relaxation characteristics of XLPE insulation, Harviliak-Negami relaxation model employing frequency domain spectroscopy data has been applied in this work. Based on the calculated model parameters α, β and τ_{hn}, the dielectric relaxation characteristics of polymeric insulation at different operating temperatures and at different water contents inside the insulation can be analyzed. Through this model, it is observed that the magnitude of α increases and β decreases with the operating temperature, whereas relaxation time constant τ_{hn} remains unchanged. Hence, it can be concluded that with the increment of temperature dielectric relaxation characteristics in XLPE deviate from Debye relaxation characteristics. In case of accumulated water content variation, it is observed that the magnitude of α and τ_{hn} decreases and β increases. Thus, it can be concluded that with the accumulation of water content inside cable insulation, dielectric relaxation characteristics of the cable gravitates towards Debye characteristics. Accumulated water creates a conducting path inside the insulation, therefore the relaxation time constant τ_{hn} decreases with the accretion of injected water content.

In this work, a methodology has been proposed to estimate water content inside XLPE cable insulation based on the FDS data. This method is a cost-effective technique for condition assessment of water tree aged cable. However, results presented in this work show that the estimation accuracy of this method is not satisfactory for in-service units that have low ppm water content.

9.2. FUTURE SCOPE:

In the present work, condition monitoring of XLPE cable is by the aforementioned models based on dielectric response measured in both time and frequency domain. This study is helpful to examine the active polarization process and dielectric relaxation characteristics inside the insulation at different conditions. Further research works that can be carried out in this area are given as follows,

- Condition based monitoring of thermally aged XLPE cable, based on the dielectric response measurement.
- Investigation of non-uniform aging in XLPE cable due to temperature gradient, by formulating modified Debye model through PDC measurement.
- Investigation of the effect of artificial defect on XLPE cable based on partial discharge measurement.
- Application of artificial intelligence to simulate water tree structure inside cable insulation and to investigate faults in that insulation.
- Localization of water tree inside XLPE cable insulation based on finite element method and frequency response analysis.

REFERENCES

1. M.Wu, B.Ouyang and W.Wu, “The frequent accidents and reasons of XLPE cable”, *Electric Power, vol. 46, no. 5, pp. 66-70, 2013.*

2. M.Dakka, A.Bulinski, and S.Bamji, “On-site diagnostics of medium-voltage underground cross-linked polyethylene cables”, *IEEE Electrical Insulation Magazine, vol. 27, no. 4, pp. 34-44, 2011.*

3. E.David, J.L.Parpal and J.P.Crine, “Aging of XLPE Cable Insulation under Combined Electrical and Mechanical Stresses”, *Proceedings of Conference Record of the 1996 IEEE International Symposium on Electrical Insulation, Montreal, Quebec, Canada, June 1996.*

4. V.Vahedy, “Polymer insulated high voltage cables”, *IEEE Electrical Insulation Magazine, vol. 22, pp. 13-18, 2006.*

5. N.Amyot, E.David, S.Y.Lee and I.H.Lee, “Influence of post-manufacturing residual mechanical stress and crosslinking by-products on dielectric strength of HV extruded cables”, *IEEE Transactions on dielectrics and electrical insulation. vol. 9, no. 3, pp. 458 – 466, June 2002.*

6. A.Harlin, M.G.Danikas and P.Hyvönen “Polyolefin insulation degradation in electrical field below critical inception voltages”, *Journal of electrical engineering, vol. 56, no. 5-6, pp. 135-140, 2005.*

7. V.Buchholz, M.Colwell, H.E.Orton and J.Y.Wong, "Elevated temperature operation of XLPE distribution cable systems", *IEEE Transactions on Power Delivery, vol. 8, no. 3, 1993.*

8. J.Densley, R.Bartnikas and B.S.Bernstein, “Multi-stress ageing of extruded insulation system for transmission cables”, *IEEE Electrical insulation magazine, vol. 9, no. 1, pp. 15-17, January/February 1993.*

9. J.P.Crine “Influence of electro-mechanical stress on electrical properties of dielectric polymers”, *IEEE Transactions on dielectrics and electrical insulation, vol. 12, no. 4, pp. 791 – 800, August 2005.*

10. G.C.Montanari, C.Laurent, G.Teyssedre, A.Campus and U.H.Nilsson, "From LDPE to XLPE: Investigating the change of electrical properties. Part I: Space charge, conduction and lifetime", *IEEE Transactions on Dielectrics and Electrical Insulation, vol. 12, no.3, pp. 438-446, Jun 2005.*

11. T.Salivon, X.Colin and R.Comte, "Degradation of XLPE and PVC cable insulators", *Proceedings of IEEE Conference on Electrical Insulation and Dielectric Phenomena (CEIDP), pp. 656-659, 2015.*

12. P.Hyvönen, "Prediction of insulation degradation of distribution power cables based on chemical analysis and electrical measurements", *Doctoral dissertation, Helsinki University of Technology, Finland, ISBN 978-951-22-9402-2, 2008.*

13. S.Hvidsten. "Nonlinear dielectric response of water treed XLPE cable insulation", *Doctoral dissertation, Norwegian University of Science and Technology, Department of electrical power engineering, ISBN 82-471-0433-4, 1999.*

14. P.Werelius, P.Thärning, R.Eriksson, B.Holmgren and U.Gäfvert, "Dielectric spectroscopy for diagnosis of water tree deterioration in XLPE cables*", IEEE Transactions on Dielectrics and Electrical Insulation, vol. 8, no.1, pp. 27-42, 2001.*

15. P. Werelius, "Development and Application of High Voltage Dielectric Spectroscopy for Diagnosis of Medium Voltage XLPE Cables," *Royal Institute of Technology (KTH), Sweden, 2001.*

16. G. Ye, H. Li, F. Lin, J. Tong, X. Wu, and Z. Huang, "Condition assessment of XLPE insulated cables based on polarization/depolarization current method," *IEEE Transactions on Dielectrics and Electrical Insulation vol. 23, no. 2, pp. 721–729, 2016.*

17. J.Òrrit, "Identification of dipolar relaxations in dielectric spectra of mid-voltage cross-linked polyethylene cables", *Journal of Electrostatics, vol. 69, pp. 119-125, 2011.*

18. B.Gracia, B.valecillos and J.C.Burgos, "Determination of Water Content in Transformer Solid Insulation by Frequency Domain Spectroscopy", *Proceedings of the 5th WSEAS/IASME International Conference on Electric Power Systems, High Voltages, Electric Machines, Tenerife, Spain, pp. 18-23, December 2005.*

19. B.Oyegoke, P.Hyvönen, M.Aro and N.Gao, "Application of dielectric response measurement on power cable systems", *IEEE Transactions on dielectrics and electrical insulation. vol. 10, no. 5. pp. 862 – 873, 2003.*

20. C.S.Pispiris, "Cable Diagnosis. In-situ Tests with Returned Voltage Diagnosis Method in Romania", *Proceedings of the 16th International Conference and Exhibition on Electricity Distribution (CIRED), no. 482, pp. 18–21, 2001.*

21. W.S.Zaengl, "Dielectric Spectroscopy in time and frequency domain for HV Power Equipment. I. Theoretical considerations", *IEEE Electrical Insulation Magazine, vol. 19, no. 5, pp. 5-19, 2003.*

22. S.Chakravorti, D.Dey and B.Chatterjee, "Recent Trends in the Condition Monitoring of Transformers", *Springer-Verlag London 2013.*

23. T. K. Saha and K. P. Mardira, "Modeling metal oxide surge arrester for the modern polarization based diagnostics", *IEEE Transactions on Dielectrics and Electrical Insulation vol. 12, no. 6, pp. 1249–1258, 2005.*

24. M. K. Pradhan, J. H. Yew, and T. K. Saha, "Influence of the geometrical parameters of power transformer insulation on the frequency domain spectroscopy measurement", *IEEE Power and Energy Society General Meeting - Conversion and Delivery of Electrical Energy in the 21st Century, pp. 1–8, 2008.*

25. S. K. Ojha, P. Purkait, and S. Chakravorti, "Modeling of relaxation phenomena in transformer oil-paper insulation for understanding dielectric response measurements", *IEEE Transactions on Dielectrics and Electrical Insulation, vol. 23, no. 5, pp. 3190–3198, 2016.*

26. N.Haque, S.Dalai, B.Chatterjee, et al., "Study on charge de-trapping and dipolar relaxation properties of epoxy resin from discharging current measurements", *IEEE Transactions on Dielectrics and Electrical Insulation, vol. 24, no. 6, pp. 3811-3820, 2017.*

27. A. Metwally, *"*The Evolution of Medium Voltage Power Cables*", IEEE Potentials, Vol. 31, No. 3, pp. 20-25, 2012.*

28. T.K.Saha, P.Purkait and F.Müller, *"*Deriving an Equivalent Circuit of Transformers Insulation for Understanding the Dielectric Response Measurements", *IEEE Transactions on Power delivery, vol. 20, no. 1, pp. 149-157, January 2005.*

29. S.Sulaiman, A.M.Ariffin and D.T.Kien, “Determining the Number of Parallel RC Branches in Polarization/Depolarization Current modeling for XLPE Cable Insulation”, *International Journal on Advanced Science Engineering Information Technology, vol. 7, no. 3, 2017.*

30. A.K.Jonscher, “Dielectric relaxation in solids”, *Journal of Physics D: Applied Physics, vol. 32, no. 14, pp. 57-70, February 1999.*

31. P.J.W.Debye, “Polar molecules”, *Chemical Catalog Company, Incorporated, 1929.*

32. K.S.Cole and R.H.Cole, “Dispersion and absorption in dielectrics I. Alternating current characteristics”, *The Journal of Chemical Physics, vol. 9, no. 4, pp. 341-351, 1941.*

33. D.W.Davidson and R.H.Cole, “Dielectric relaxation in glycerol, propylene glycol, and n-propanol”, *The Journal of Chemical Physics, vo. 19, no. 12, pp. 1484-1490, 1951.*

34. S.Havriliak and S.Negami, “A complex plane analysis of α-dispersions in some polymer systems”, *Journal of Polymer Science Part C: Polymer Symposia, vol. 14, no. 1, pp. 99-117, 1966.*

35. S.K.Ojha, P.Purkait, B.Chatterjee and S.Chakravorti, “Application of Cole–Cole model to transformer oil-paper insulation considering distributed dielectric relaxation”, *IET Science, High voltage, vol. 4, no. 1, pp. 72-79, March 2019.*

36. *G.*Meier and A.Saupe, “Dielectric Relaxation in Nematic Liquid Crystals”, *Journal of Molecular Crystals, vol. 1, no. 4, pp. 515-525, 1965*

37. A.Alegria and J.Colmenero, “Dielectric relaxation of polymers: segmental dynamic sunder structural constrains”, *Soft Matter, vol. 12, no. 37, pp. 7709-7725, 2016.*

38. D.Gorinevsky, “An approach to parametric nonlinear least square optimization and application to task-level learning control”, *IEEE Transactions on Automatic Control, vol. 42, no. 7, pp. 912-917, 1997.*

39. A.Kumar, H.C.Verma, A.Baral, A.K.Pradhan and S.Chakravorty, "Estimation of paper-moisture in transformer insulation employing dielectric spectroscopy data", *IET Science, Measurement & Technology, vol. 12, no. 4, pp-536-541, 2018.*

40. W.S.Zaengl, “Applications of dielectric spectroscopy in time and frequency domain for HV power equipment”, *IEEE Electrical Insulation Magazine, vol. 19, no. 6, pp. 9–22, 2003.*